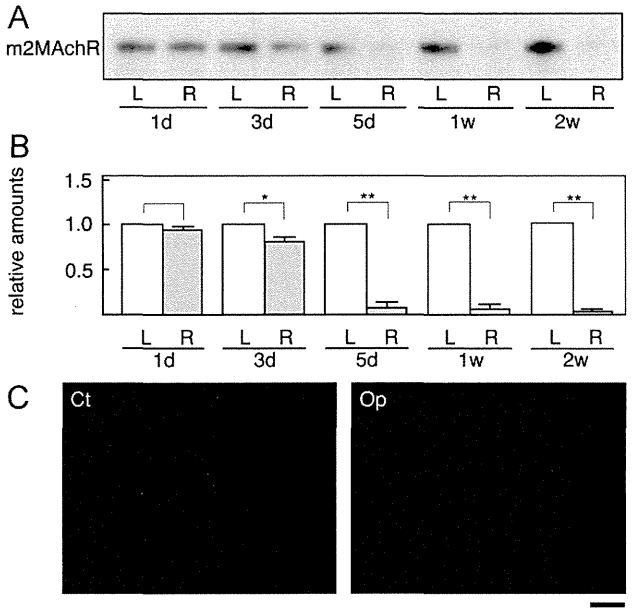

Fig. 3 – Response of m2MAchR to facial nerve transection. Sets of contralateral (L) and ipsilateral (R) facial nuclei recovered at 1, 3, 5, 7 and 14 days after transection were immunoblotted for m2 muscarinic acetylcholine receptor (m2MAchR) (A). The intensity of the m2MAchR bands in A was determined by a densitometer, and the value of transected facial nucleus (R) was expressed as a value relative to that of control nucleus (L). Data shown are means ± SDs from three independent experiments (*$P<0.05$, **$P<0.01$) (B). Brainstem sections obtained at 5 days after transection were immunohistochemically stained with anti-m2MAchR antibody according to the fluorescence method (C). The receptor proteins were visualized by Alexa Fluor 568 (red). Control (Ct) and injured (Op) sides are shown at left and right, respectively. Scale bar = 100 μmm.

most of the anti-ChAT antibody-positive motoneurons expressed m2MAchR (Fig. 4B, ChAT vs. m2MAchR), demonstrating that the m2MAchR protein is expressed in motoneurons in the facial nucleus, as has been suggested by Hoover et al. (1996).

Accordingly, the decrease of m2MAchR levels in ipsilateral facial motoneurons was found to lag behind the reduction of ChAT, suggesting that ChAT and m2MAchR are distinctly regulated in injured motoneurons.

2.4. *Survivability of injured motoneurons*

It is generally accepted that peripheral motoneurons in adult rats do not die when they are transected. However, the reductions of ChAT (Fig. 1), VAchT (Fig. 2) and m2MAchR (Fig. 3) in the injured facial nucleus suggested the possibility that motoneurons in the ipsilateral nucleus may have died. The question of whether motoneuron cell death occurs was ascertained histochemically. The brainstem sections prepared at 5 days and 14 days after injury were stained by Nissl staining (Fig. 5A). The motoneurons in the control and transected facial nuclei appeared to be almost equally stained (Fig. 5A).

The number of motoneurons stained by Nissl staining was compared between the control and injured facial nucleus (Fig. 5B). In the facial nucleus 5 days post-injury, the average number on the control side was 114 ± 6/section, while that of the injured side was 110 ± 7/section, with no significant difference between them (Fig. 5B, left). Similarly, there was no statistical difference between the control (115 ± 4/section) and injured (111 ± 5/section) nucleus of rats at 14 days post-injury (Fig. 5B, right hand). Thus, as has been generally believed, our results indicate that transected facial motoneurons of adult rats are almost all alive at the time when ChAT, VAchT and m2MAchR levels are down-regulated.

2.5. *Changes of ChAT, VAchT and m2MAchR levels at later stage*

In addition to the early response of motoneurons to nerve injury, we analyzed it at a later stage such as 3, 4 and 5 weeks after injury (Fig. 6). Western blotting indicated that the levels of ChAT in the transected nucleus are lower than those in the control nucleus for up to 3 weeks. However, at 4–5 weeks after transection the levels had recovered to control levels (Fig. 6A, left). Quantification of the results in Western blotting clarified that the levels in the injured nucleus almost completely returned to the control levels (98 ± 10% at 5 week) (Fig. 6A, right). The levels of VAchT in the injured nucleus also returned to the control levels at 4–5 weeks post-insult, with a value of 96 ± 5% (Fig. 6B).

In the case of m2MAchR, however, the reduced levels on the transected side did not return to the original levels during 5 weeks (Fig. 6C).

3. Discussion

In the rat facial nerve injury system, it is possible to compare the expression levels of a specific protein in the ipsilateral nucleus and the contralateral nucleus. We have previously measured changes of urokinase activity (Nakajima et al., 1996, 2005), macrophage-colony stimulating factor (M-CSF)/receptor for M-CSF (cFms)/proliferating cell nuclear antigen (Yamamoto et al., 2010) and cyclin/Cdks levels (Yamamoto et al., 2012) in rat facial nerve injury. In the present study, we quantitatively traced the time-course alterations in injured facial motoneurons to obtain precise information regarding functional changes in motoneurons after insult.

So far, ChAT is well known to be expressed in human facial motoneurons (Yew et al., 1996) and rat facial motoneurons (Ichikawa et al., 1997). VAchT has also been reported to be expressed in motoneurons of the rat facial nucleus (Gilmor et al., 1996). Thus, these molecules could be used as functional markers of motoneurons.

In addition, the acetylcholine receptor was examined as a marker of the cholinergic system in the facial nucleus. Although acetylcholine receptors are divided into two groups, nicotinic and muscarinic, based on pharmacological properties, m2MAchR (Caulfield and Birdsall, 1998) was selected, because m2MAchR mRNA has been found to be located in the facial motoneurons (Hoover et al., 1996). Thus, this m2MAchR was also used as a functional marker for motoneurons.

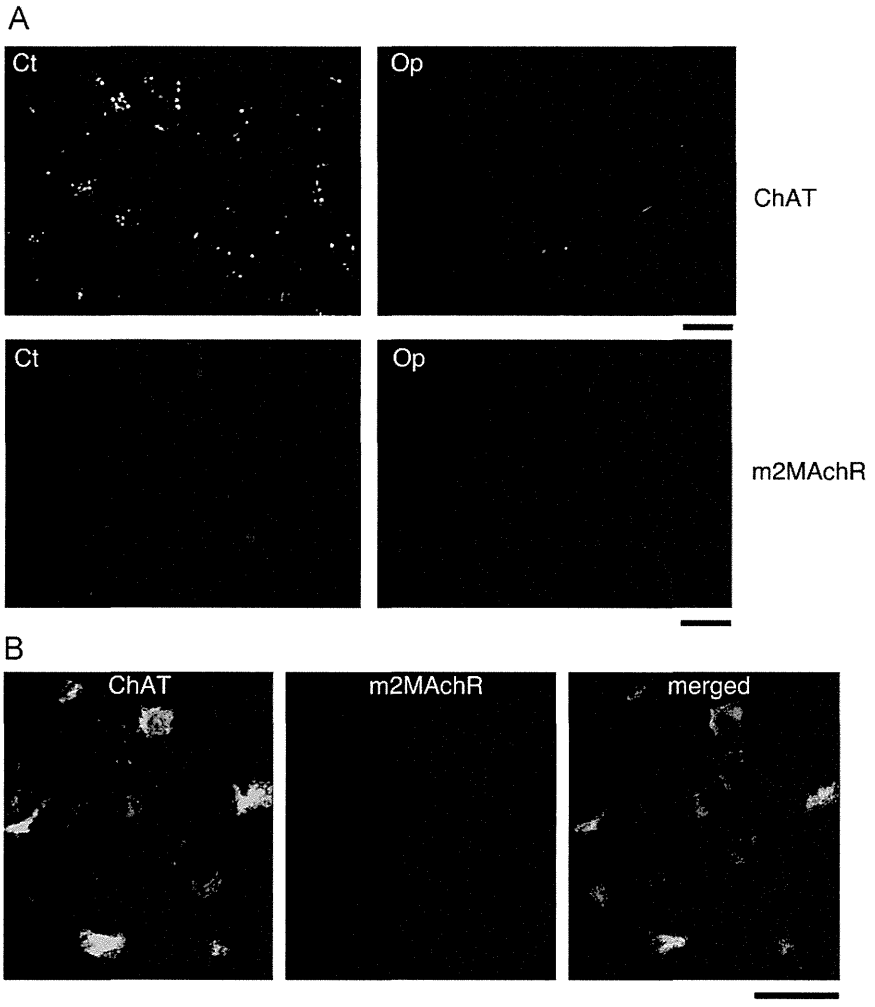

Fig. 4 – Immunohistochemical staining for ChAT and m2MAchR. The brainstem sections at 3 days after transection were stained with anti-ChAT (upper panels) antibody and anti-m2MAchR antibody (lower panels) (A). ChAT and m2MAchR were visualized by Alexa Fluor 488 (green) and Alexa Fluor 568 (red), respectively. Control (Ct) and transected (Op) sides are shown at left and right, respectively. Scale bar=50 μmm. A control facial nucleus was dually stained with anti-ChAT antibody and anti-m2MAchR antibody, and it was shown in B. ChAT and m2MAchR were visualized by Alexa Fluor 488 (green) and Alexa Fluor 568 (red), respectively. The merged image is shown on the right. Scale bar=50 μmm.

In the previous facial motoneuron injury model, biochemical and immunohistochemical analyses were carried out at 2 weeks after injury, and indicated that ChAT activity and [^{3}H]quinuclidinyl benzilate-binding activity (muscarinic acetylcholine receptor levels) were reduced in the injured motoneurons (Hoover and Hancock, 1985). In addition, the olivocochlear neurons, with the same origin as the facial motoneurons (Bruce et al., 1997), have shown a reduction in acetylcholine receptor levels when lesioned (Jin and Godfrey, 2006). These studies suggested that ChAT and muscarinic acetylcholine receptor levels are down-regulated in injured facial motoneurons. However, information regarding changes in the levels of ChAT and m2MAchR proteins in injured motoneurons is limited, and changes of VAchT protein levels are not known. Thus, in this study, to elucidate accurately the state of injured motoneurons, we determined the levels of ChAT, VAchT and m2MAchR proteins in transected facial nuclei at early (1–14 days) and later stages (3–5 weeks) post-injury.

At the early stage, ChAT protein levels in the ipsilateral nucleus were found to drop significantly (Fig. 1), as has been previously shown by RNase protection assay (Wang et al., 1997) and immunohistochemistry (Chang et al., 2004) in transected hypoglossal motoneurons. VAchT protein levels in injured facial nuclei were also recognized to drop remarkably in the same time course (Fig. 2), similar to the result by in situ hybridization in transected hypoglossal nucleus (Matsuura et al., 1997). In the axotomized facial nucleus, these ChAT and VAchT levels were down-regulated starting 1 day after transection and the depressed levels lasted for 14 days. On the other hand, m2MAchR levels in the transected nucleus were for the most part sustained (82%) up to 3 days after insult, but dropped markedly at 5 days and remained low thereafter (Fig. 4A). The delayed response of m2MAchR compared to that of ChAT was demonstrated in both the time-course experiment (Fig. 4A and B) and the immunohistochemical analyses (Fig. 5).

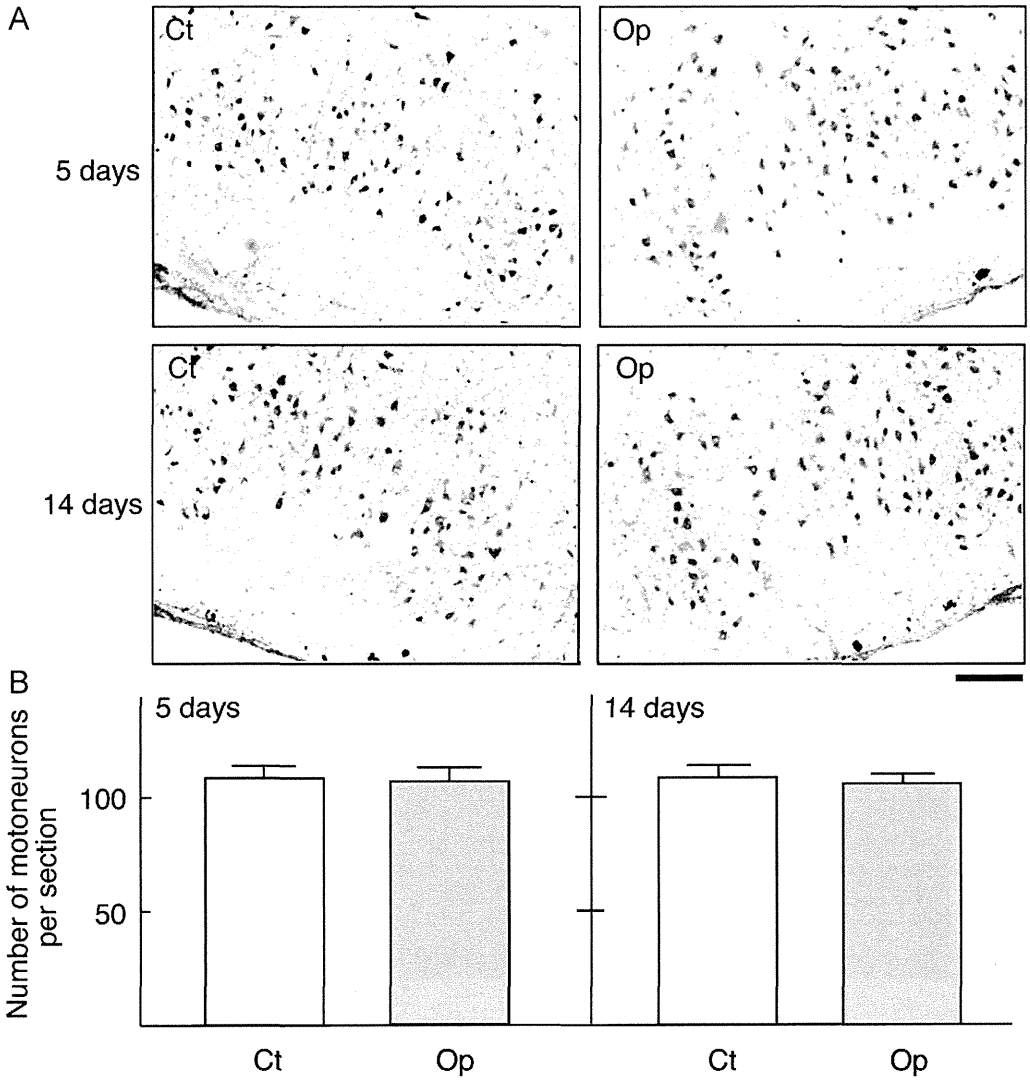

Fig. 5 – Nissl stainings of facial nuclei. Brainstem sections recovered at 5 days (upper panels) and 14 days (lower panels) after transection were subjected to Nissl staining. Control (Ct) and transected (Op) sides are shown on the left and right, respectively (A). Scale bar=200 μmm. Five cryosections around the center of the facial nucleus prepared at 5 days and 14 days post-insult were stained by Nissl-staining. The number of Nissl-staining-positive neurons was statistically compared between the control (Ct) and injured facial nucleus (Op) (B). Data shown are means±SDs from three independent experiments ($^{*}P<0.05$, $^{**}P<0.01$).

There are cases in which axotomized motoneurons die. When the facial nerves of newborn rats were transected, most of the motoneurons died (Yan et al., 1995; Graeber et al., 1998). The proportion of motoneuronal cell death occurring in axotomized motoneurons tends to decrease depending on the time after birth. Although neuronal cell death may not occur in adult age, the possibility was checked by histochemical methods. Nissl staining (Konigsmark, 1970) showed that there is no significant difference in the number of motoneurons between the contralateral and ipsilateral nucleus at 5 and 14 days after insult (Fig. 5), similar to the results by Kou et al. (1995). Being alive is very important for neurons even if they are suffering from functional depression, because only surviving neurons can regenerate later. The functionally depressed motoneurons may be in a state in which they focus on mere survival for the sake of future regeneration. The increases in the injured facial motoneurons of stearoyl-CoA desaturase involved in energy storage (Schmitt et al., 2003), and neuron-specific enolase involved in glycolysis (Angelov et al., 1994), may contribute to the reactivation/restoration of injured motoneurons.

It was actually anticipated that the injured motoneurons have restored functionality in the later stage after insult. Thus, the levels of ChAT, VAchT and m2MAchR were investigated at 3, 4 and 5 weeks after insult. ChAT levels in the ipsilateral nucleus were observed to recover to those of the control side (Fig. 6A). Similarly, restoration of ChAT levels in injured motoneurons has been reported in hypoglossal axotomy systems. Using immunohistochemical methods, Lams et al. (1988), Armstrong et al. (1991) and Rende et al. (1995) indicated the recovery of ChAT levels at 4–5 weeks post-axotomy. Matsuura et al. (1997) also reported later restoration of ChAT according to an in situ hybridization method.

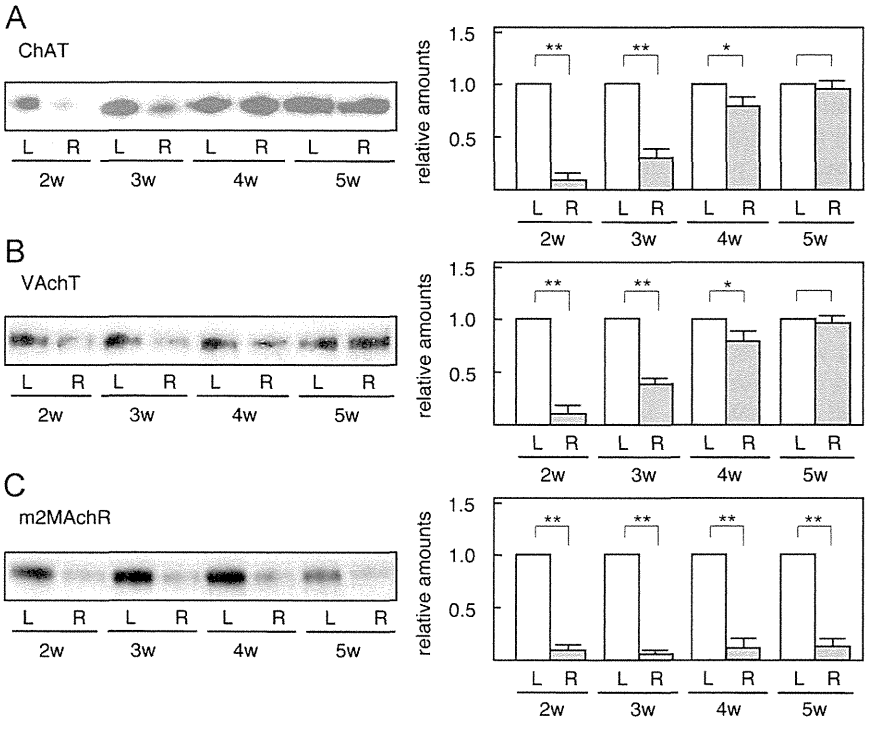

Fig. 6 – Levels of ChAT, VAchT and m2MAchR at later stage. Sets of contralateral (Left side; L) and ipsilateral (Right side; R) facial nuclei recovered at 3, 4 and 5 weeks after axotomy were immunoblotted for ChAT (A), VAchT (B) and m2MAchR (C). The facial nuclei removed at 2 weeks after injury were simultaneously analyzed. The intensity of the bands in A, B and C was determined by a densitometer, and the value of the transected facial nucleus (R) was expressed as the value relative to that of the control nucleus (L). The data on the right are means ± SDs from three independent experiments ($^{*}P<0.05$, $^{**}P<0.01$).

Likewise, VAchT levels in the transected facial nucleus returned to control levels during at 4–5 weeks after injury (Fig. 6B). However, distinct from ChAT and VAchT, m2MAchR levels in ipsilateral nucleus had not returned to the control levels even at 5 weeks after insult (Fig. 6C). It is most likely that the expression/degradation of ChAT/VAchT and m2MAchR is individually regulated in injured motoneurons.

Collectively, the levels of ChAT and VAchT were found to be down-regulated in transected motoneurons almost immediately (Days 1–3) after injury, while m2MAchR levels were recognized to decrease starting Day 5 after insult. Although the m2MAchR sustained the low levels for 5 weeks after injury, ChAT and VAchT were recovered in the later stage (Weeks 4–5).

4. Experimental procedures

4.1. *Antibodies and reagents*

The antibodies against choline acetyltransferase (ChAT) and vesicular acetylcholine transporter (VAchT) were obtained from Millipore Corporation (Temecula, CA). The antibodies against the m2 muscarinic acetylcholine receptor (m2MAchR) and NMDA receptor 3B subunit (NR3B) were obtained from Abcam (Cambridge, UK). The antibody against ionized Ca^{2+} binding adapter molecule 1 (Iba1; Imai et al., 1996) was obtained from Wako Pure Chemical Industries (Osaka, Japan).

Horseradish peroxidase (HRP)-conjugated anti-rabbit IgG, HRP-conjugated anti-mouse IgG, HRP-conjugated anti-goat IgG and HRP-conjugated anti-guinea pig IgG were purchased from Santa Cruz Biotechnology (Santa Cruz, CA). Alexa Fluor 488-conjugated anti-mouse IgG, Alexa 568-conjugated anti-goat IgG and Alexa 568-conjugated anti-rabbit IgG were purchased from Invitrogen Corporation (Carlsbad, CA). For light microscopic immunohistochemical staining, we used a Vectastain ABC kit (Vector Laboratories, Inc., Burlingame, CA).

Cresyl violet for Nissl staining was obtained from Sigma-Aldrich (Tokyo, Japan).

4.2. *Animals and transection of facial nerve*

Male rat littermates (8 weeks) were prepared for the time-course experiment and kept on a 12-h daylight cycle with food and water. They were cared for in accordance with the guidelines of the ethics committee of Soka University.

For immunoblotting and immunohistochemical studies, the right facial nerve of rats was transected at the stylomastoid foramen under diethyl ether anesthesia, as described previously (Nakajima et al., 1996; Graeber et al., 1998). The rats were decapitated at early time points (1, 3, 5, 7, and 14 days) or later time points (3, 4, and 5 weeks) under anesthesia, and their whole brains were removed, frozen on dry ice, and stored at −80 °C until use.

4.3. *Immunoblotting*

The brainstem was chipped from the hind portion to the depth of the facial nucleus. The contralateral and ipsilateral

facial nuclei were carefully cut out from the frozen brainstem. The cut facial nuclei were solubilized by sonication with nonreducing Laemmli's sample solution [62.5 mM Tris HCl (pH 6.8), 2% sodium dodecyl sulfate (SDS), and 5% glycerol] and centrifuged at 100,000 *g* for 30 min. An aliquot of the supernatant was taken for protein determination. The protein contents were determined according to the method of Lowry et al. (1951) with bovine serum albumin as a standard. The remaining supernatant was adjusted to contain 2.5% 2-mercaptethanol and was heated at 90 °C for 3 min.

The resultant samples were subjected to SDS-polyacrylamide gel electrophoresis (PAGE) with 4–20% polyacrylamide gel, and immunoblotting following PAGE was carried out as reported previously (Yamamoto et al., 2010). The blotted Immobilon (Millipore Corporation, Bedford, MA) was blocked with TNw buffer [10 mM Tris–HCl (pH 7.5), 150 mM NaCl, and 0.01% Tween 20] containing 3% skim milk (3SM/TNw) for 1 h, and incubated with primary antibody (1:1000 for ChAT, VAchT, and m2MAchR; 1:500 for NR3B) in 3SM/TNw at 4 °C overnight. After the membrane was rinsed five times with TNw buffer, it was incubated with HRP-conjugated anti-rabbit IgG antibody, HRP-conjugated anti-mouse IgG antibody, HRP-conjugated anti-goat IgG antibody or HRP-conjugated anti-guinea pig IgG antibody (1:1000) for 3 h at room temperature. After sufficient rinsing, the antigen–antibody complex on the membrane was detected with an enhanced chemiluminescence system. If necessary, the membranes were re-proved.

4.4. *Immunohistochemistry*

The brainstem was cut into 20-μm-thick sections with a cryostat at the level of the facial nuclei (Graeber et al., 1998). These sections were air-dried for 20 min and fixed in 3.7% paraformaldehyde and 0.9% NaCl/0.1 M phosphate buffered solution (PBS; pH 7.4) for 5 min. Subsequently, they were treated sequentially with 50% acetone for 2 min, 100% acetone for 3 min and 50% acetone for 2 min, and further with 0.05% TritonX-100/10 mM PBS containing 0.9% NaCl (10 mM PBS-NaCl) for 5 min. These sections were blocked with blocking solution (2% skim milk/10 mM PBS-NaCl) for 1 h at room temperature.

For the avidin–biotin–peroxidase complex (ABC) method, the cryosections were incubated with anti-ChAT antibody (1:100) at 4 °C overnight, and then with biotinylated secondary antibody (1:200) for 1 h. The antigens on the sections were finally detected by adding 0.001% H_2O_2 and 0.08 mM diaminobenzidine as reported previously (Yamamoto et al., 2010).

For dual fluorescent staining, the cryosections were separately incubated with two primary antibodies at 4 °C overnight, and subsequently with two fluorescence-conjugated secondary antibodies for 3 h at room temperature. Anti-ChAT (1:200), anti-NR3B (1:500) and anti-m2MAchR (1:100) antibodies were used as the primary antibodies. Alexa Fluor 488-conjugated anti-mouse IgG (1:100), Alexa Fluor 568-conjugated anti-goat IgG (1:100) and Alexa Fluor 568-conjugated anti-rabbit IgG (1:200) were used as secondary antibodies. In the case of single fluorescence staining, the cryosections were incubated with a primary antibody at 4 °C overnight and then with a suitable secondary antibody for 3 h at room temperature.

The stained sections were dehydrated and mounted, and observed by biological microscope or fluorescent microscope.

4.5. *Histochemistry*

After dehydration and rehydration, the brainstem sections were stained with 0.5% cresyl violet/1 M acetate buffer (pH 3.9) according to Nissl staining methods (Konigsmark, 1970). These specimens were mounted after dehydration.

4.6. *Statistical analysis*

The densities of the bands of ChAT, VAchT and m2MAchR in the immunoblotting were measured by densitometer and expressed as means ± SDs of three to four independent experiments. Differences between the contralateral and ipsilateral nucleus were assessed via Student's t-test. In all cases, P values less than 0.05 were considered to be significant ($^{*}P<0.05$, $^{**}P<0.01$).

Acknowledgments

This work was supported by a Grant-in-Aid for Scientific Research (C) from Japan Society for the Promotion of Science.

REFERENCES

Angelov, D.N., Neiss, W.F., Gunkel, A., Guntinas-Lichius, O., Stennert, E., 1994. Axotomy induces intranuclear immunolocalization of neuron-specific enolase in facial and hypoglossal neurons of the rat. J. Neurocytol. 23, 218–233.

Armstrong, D.M., Brady, R., Hersh, LB., Hayes, R.C., Wiley, R.G., 1991. Expression of choline acetyltransferase and nerve growth factor receptor within hypoglossal motoneurons following nerve injury. J. Comp. Neurol. 304, 596–607.

Brown, D.A., 2010. Muscarinic acetylcholine receptors (mAChRs) in the nervous system: some functions and mechanisms. J. Mol. Neurosci. 41, 340–346.

Bruce, L.L., Kingsley, J., Nichols, D.H., Fritzsch, B., 1997. The development of vestibulocochlear efferents and cochlear afferents in mice. Int. J. Dev. Neurosci. 15, 671–692.

Caulfield, M.P., Birdsall, N.J.M., 1998. International Union of Pharmacology. XVII Classification of muscarinic acetylcholine receptors. Pharmacol. Rev. 50, 279–290.

Chang, H.M., Wei, I.H., Tseng, C.Y., Lue, J.H., Wen, C.Y., Shieh, J.Y., 2004. Differential expression of calcitonin gene-related peptide (CGRP) and choline acetyltransferase (ChAT) in the axotomized motoneurons of normoxic and hypoxic rats. J. Chem. Neuroanat. 28, 239–251.

Eiden, L.E., 1998. The cholinergic gene locus. J. Neurochem. 70, 2227–2240.

Engel, A.G., Ohno, K., Sine, S.M., 2003. Congenital myasthenic syndromes: progress over the past decade. Muscle Nerve 27, 4–25.

Gilmor, M.L., Nash, N.R., Roghani, A., Edwards, R.H., Yi, H., Hersch, S.M., Levey, A.I., 1996. Expression of the putative vesicular acetylcholine transporter in rat brain and localization in cholinergic vesicles. J. Neurosci. 16, 2179–2190.

Graeber, M.B., Lopes-Redondo, F., Ikoma, E., Ishikawa, M., Imai, Y., Nakajima, K., Kreutzberg, G.W., Kohsaka, S., 1998. The microglia/macrophage response in the neonatal rat facial nucleus following axotomy. Brain Res. 813, 241–253.

Haas, C.A., Donath, C., Kreutzberg, G.W., 1993. Differential expression of immediate early genes after transection of the facial nerve. Neuroscience 53, 91–99.

Hersh, L.B., 1982. Kinetic studies of the choline acetyltransferase reaction using isotope exchange at equilibrium. J. Biol. Chem. 257, 12820–12825.

Hoover, D.B., Baisden, R.H., Lewis, J.V., 1996. Axotomy-induced loss of m2 muscarinic receptor mRNA in the rat facial motor nucleus precedes a decrease in concentration of muscarinic receptors. J. Histochem. 28, 771–778.

Hoover, D.B., Hancock, J.C., 1985. Effect of facial nerve transection on acetylcholinesterase, choline acetyltransferase and [^{3}H]quinuclidinyl benzilate binding in rat facial nuclei. Neuroscience 15, 481–487.

Ichikawa, T., Ajiki, K., Matsuura, J., Misawa, H., 1997. Localization of two cholinergic markers, choline acetyltransferase and vesicular acetylcholine transporter in the central nervous system of the rat: in situ hybridization histochemistry and immunohistochemistry. J. Chem. Neuroanat. 13, 23–39.

Imai, Y., Ibata, I., Ito, D., Ohsawa, K., Kohsaka, S., 1996. A novel gene iba1 in the major histocompatibility complex class III region encoding an EF hand protein expressed in a monocytic lineage. Biochem. Biophys. Res. Commun. 224, 855–862.

Jin, Y-M., Godfrey, D.A., 2006. Effects of cochlear ablation on muscarinic acetylcholine receptor binding in the rat cochlear nucleus. J. Neurosci. Res. 83, 157–166.

Konigsmark, B.W., 1970. Methods for counting of neurons. In: Nauta, W.J.H, Ebbesson, S.O.E. (Eds.), Contemporary Research Methods in Neuroanatomy. Springer, Berlin Heidelberg New York, pp. 315–340.

Kreutzberg, G.W., 1996. Microglia: a sensor for pathological events in the CNS. Trends Neurosci. 19, 312–318.

Kou, S.Y., Chiu, A.Y., Patterson, P.H., 1995. Differential regulation of motor neuron survival and choline acetyltransferase expression following axotomy. J. Neurobiol. 27, 561–572.

Lams, B.E., Isacson, O., Sofroniew, M.V., 1988. Loss of transmitter-associated enzyme staining following axotomy does not indicate death of brainstem cholinergic neurons. Brain Res. 475, 401–406.

Lowry, O.J., Rosebrough, N.J., Farr, A.L., Randall, R.J., 1951. Protein measurement with the Folin phenol reagent. J. Biol. Chem. 193, 265–275.

Matsuda, K., Fletcher, M., Kamiya, Y., Yuzaki, M., 2003. Specific assembly with the NMDA receptor 3B subunit controls surface expression and calcium permeability of NMDA receptors. J. Neurosci. 23, 10064–10073.

Matsuura, J., Ajiki, K., Ichikawa, T., Misawa, H., 1997. Changes of expression levels of choline acetyltransferase and vesicular acetylcholine transporter mRNAs after transection of the hypoglossal nerve in adult rats. Neurosci. Lett. 236, 95–98.

Moran, L.B., Graeber, M.B., 2004. The facial nerve axotomy model. Brain Res. Rev. 44, 154–178.

Nakajima, K., Reddington, M., Kohsaka, S., Kreutzberg, G.W., 1996. Induction of urokinase-type plasminogen activator in rat facial nucleus by axotomy of facial nerve. J. Neurochem. 66, 2500–2505.

Nakajima, K., Tohyama, Y., Kurihara, T., Kohsaka, S., 2005. Axotomy-dependent urokinase induction in the rat facial nucleus: possible stimulation of microglia by neurons. Neurochem. Int. 46, 107–116.

Rende, M., Giambanco, I., Buratta, M, Tonali, P., 1995. Axotomy induces a different modulation of both low-affinity nerve growth factor receptor and choline acetyltransferase between adult rat spinal and brainstem motoneurons. J. Comp. Neurol. 363, 249–263.

Schmitt, A.B., Breuer, S., Liman, J., Buss, A., Schlangen, C., Pech, K., Hol, E.M., Brook, G.A., Noth, J., Schwaiger, F.W., 2003. Identification of regeneration-associated genes after central and peripheral nerve injury in the adult rat. BMC Neurosci. 4, 8.

Tetzlaff, W., Kreutzberg, G.W., 1984. Enzyme changes in the rat facial nucleus following a conditioning lesion. Exp. Neurol. 85, 547–564.

Wang, W., Salvaterra, P.M., Loera, S., Chiu, A.Y., 1997. Brain-derived neurotrophic factor spares choline acetyltransferase mRNA following axotomy of motor neurons in vivo. J. Neurosci. Res. 47, 134–143.

Yamamoto, S., Kohsaka, S., Nakajima, K., 2012. Role of cell-cycle associated proteins in axotomized rat facial nucleus. Glia 60, 570–581.

Yamamoto, S., Nakajima, K., Kohsaka, S., 2010. Macrophage-colony stimulating factor (M-CSF) as an inducer of microglial proliferation in axotomized rat facial nucleus. J. Neurochem. 115, 1057–1067.

Yan, Q., Matheson, C., Lopez, O.T., 1995. In vivo neurotrophic effects of GDNF on neonatal and adult facial motor neurons. Nature 373, 341–344.

Yao, W., Godfrey, D.A., 1999. Vesicular acetylcholine transporter in the rat cochlear nucleus: an immunohistochemical study. J. Histochem. Cytochem. 47, 83–90.

Yew, D.T., Webb, S.E., Lam, E.T., 1996. Neurotransmitters and peptides in the developing human facial nucleus. Neurosci. Lett. 206, 65–68.

GLIA

GLIA 61:47–54 (2013)

Purinergic Receptors in Microglia: Functional Modal Shifts of Microglia Mediated by P2 and P1 Receptors

SCHUICHI KOIZUMI,[1,2] KEIKO OHSAWA,[3] KAZUHIDE INOUE,[4] AND SHINICHI KOHSAKA[3]*

[1]*Department of Neuropharmacology, Graduate School of Medicine and Engineering, University of Yamanashi, Yamanashi 409-3898, Japan*

[2]*Japan Science and Technology Agency, Core Research for Evolutional Science and Technology, Tokyo, Japan*

[3]*Department of Neurochemistry, National Institute of Neuroscience, 4-1-1 Ogawahigashi Kodaira, Tokyo 187-8502, Japan*

[4]*Department of Molecular System Pharmacology, Graduate School of Pharmaceutical Sciences, Kyushu University, 3-1-1 Maidashi, Fukuoka 812-8521, Japan*

KEY WORDS

modal shift; crosstalk; process extension; migration; phagocytosis

ABSTRACT

Microglia are sensitive to environmental changes and are immediately transformed into several phenotypes. For such dynamic "modal shifts", purinergic receptors have central roles. When microglia sense ATP/ADP leaked from injured cells by $P2Y_{12}$ receptors, they are transformed into a moving phenotype, showing process extension and migration toward the injured sites. Microglia upregulate adenosine A_{2A} receptors, by which they retract the processes showing an amoeboid-shaped, activated phenotype. Microglia also upregulate $P2Y_6$ receptors, and if they meet UDP leaked from dead cells, microglia start to engulf and eat the dead cells as a phagocytic phenotype. The $P2Y_{12}$ receptor-mediated responses are modulated by other P2 or P1 receptors. In contrast, the $P2Y_6$ receptor-mediated responses were not influenced by $P2Y_{12}$ receptors and vice versa. Microglia appear to use purinergic signals either cooperatively or distinctively to cause their modal shifts.

INTRODUCTION

In the normal healthy adult brain, microglia are present in a so-called "resting form" with highly branched processes and thus are called "ramified microglia". Although resting microglia were thought to be quiescent, recent studies have shown that they are highly motile (Davalos et al., 2005; Nimmerjahn et al., 2005) and actively survey their environment using the branched processes, and thus they are also called "surveying" microglia (Tremblay et al., 2011; Wake et al., 2009). Surveying microglia show constantly and rapidly moving processes but largely invariant soma positions in the healthy brain. They look as if they are patrolling or monitoring their own territories by the processes. Microglia are very sensitive to environmental changes in the brain, and when they sense unusual signs in several neurodegenerative diseases or traumatic injuries with the motile processes, they immediately transform their phenotypes from surveying into activated forms. The term "activated microglia" includes several different phenotypes, each of which is generally associated with very active motilities with highly complex spatiotemporal patterns.

In this review, we focus on research within the past several years regarding the purinoceptor-mediated dynamic functional changes or "functional modal shift" of microglia. We especially emphasize that microglia distinguish among multiple purinoceptors and transform themselves into appropriate phenotypes. Microglia in pathological brains show several functional phenotypes, such as process extension, migration, proliferation, and phagocytosis (Hanisch and Kettenmann, 2007; Kreutzberg, 1996; Nakajima et al., 1996). For such phenotypes, the release of leakage of extracellular nucleotides/nucleosides from injured or dead cells and activation of the corresponding purinoceptors (P2 or P1 receptors) have central roles. When cells are injured or dead, they release or leak a large amount of nucleotides, some of which are immediately degraded into nucleosides by ecto-nucleotidases (ENTPDases), such as CD39 and CD73/5′-nucleotidase enzymes (Robson et al., 2006). Thus, microglia could be exposed to both nucleotides and nucleosides, and receive both signals because they possess multiple P2 and P1 receptors. Importantly, the expression levels of these receptors show complex spatiotemporal patterns according to changes in their microenvironment. Microglia seem to use these signals cooperatively or distinctively, and control complex and dynamic changes of microglial phenotypes. For example, microglia protrude their processes and migrate toward injured sites, when triggered by extracellular ATP/ADP and the activation of $P2Y_{12}$ receptors. The $P2Y_{12}$ receptor-mediated responses are modulated by the activation of some other P2 and P1 receptors, suggesting an intimate cross-

*Correspondence to: Shinichi Kohsaka, Department of Neurochemistry, National Institute of Neuroscience, 4-1-1 Ogawahigashi, Kodaira, Tokyo 187-8502, Japan. E-mail: kohsaka@ncnp.go.jp

Received 21 April 2012; Accepted 30 April 2012

DOI 10.1002/glia.22358

Published online 1 June 2012 in Wiley Online Library (wileyonlinelibrary.com).

talk among purinergic receptors. Microglia phagocytose the dead cells or debris when they sense UDP by $P2Y_6$ receptors. Interestingly, the $P2Y_6$ receptor-mediated responses are not affected by the activation of $P2Y_{12}$ receptors and vice versa, suggesting that eating and migrating behaviors are distinctively controlled by different purinergic receptors. Such cooperative or distinct purinergic signals appear to have indispensable roles in triggering the dynamic and complex modal shift of microglia.

MICROGLIAL PURINERGIC RECEPTORS

The purinergic system has ancient evolutionary roots and is operative in almost all tissues (Burnstock, 2006; Burnstock et al., 2011; Burnstock and Verkhratsky, 2009). In the CNS, this system is especially important because both purines and pyrimidines act as extracellular molecules that mediate interglial and neuron-to-glia interactions. ATP, the primary nucleotide in the CNS, regulates various physiological functions of microglia (Inoue, 2002; Kettenmann et al., 2011; Sperlagh and Illes, 2007). Microglia express multiple functional purinergic receptors. With regard to P2 receptors, they express both ionotropic P2X and metabotropic P2Y receptors, including $P2X_4$, $P2X_7$, $P2Y_2$, $P2Y_4$, $P2Y_6$, $P2Y_{12}$, and $P2Y_{14}$ receptors (Boucsein et al., 2003; James and Butt, 2002; Kobayashi et al., 2006; Koizumi et al., 2007; Sasaki et al., 2003; Tsuda et al., 2003). With regard to P1 receptors, microglia express all subclasses of adenosine receptors, i.e., adenosine A_1, A_{2A}, A_{2B}, and A_3 receptors (Fredholm et al., 2001). Although microglia express multiple P2 and P1 receptors, some of which could be activated simultaneously, the expression levels of these receptors are largely dependent on their environment and, thus, the set of purinergic receptors varies according to microglial phenotypes. In addition, some sets of receptors might be activated simultaneously causing cooperative effects, whereas others might function independently. Thus, microglia alter the purinergic system according to circumstances, and transform themselves into various phenotypes.

SURVEYING AND PROCESS-EXTENDING MICROGLIA

Recent accumulating evidence has shown that astrocytes can regulate synaptic transmissions by responding to neurotransmitters and releasing gliotransmitters (Halassa and Haydon, 2010; Haydon, 2001; Koizumi et al., 2003; Perea and Araque, 2010). However, whether microglia influence synaptic transmission in similar ways is unclear. As already mentioned, the processes of ramified microglia in adult healthy brains show rapid and continuous motions, by which they survey their microenvironment (Davalos et al., 2005; Nimmerjahn et al., 2005), including synapses (Wake et al., 2009). Interestingly, microglia make direct contact with synapses at a frequency of about once per hour, which is dependent on the neuronal excitability (Wake et al., 2009), suggesting that there could be an intimate communication between neurons and microglia at synapses, by which surveying behaviors are controlled. Microglia express several transmitter receptors, including P2 receptors, and the base motility of microglia is at least partly dependent on the extracellular ATP/ADP (Davalos et al., 2005). Thus, similar to astrocytes, microglia can sense neuronal activity (Pocock and Kettenmann, 2007) and possibly send diffusible molecules to the synapses or astrocytes (Pascual et al., 2011) as synaptic partners. Purinergic systems would be important for understanding the molecular mechanisms of synapse-to-microglia interaction as well as the surveying behaviors of microglia, but further intensive studies are required to clarify these issue.

When acute brain injuries occur, microglia dramatically increase their motilities and are transformed into a process-extending phenotype. They immediately extrude processes to the injured site, by which they prevent the spread of the lesion in the brain (Hines et al., 2009). The process extension of microglia did not occur in the brain of $P2Y_{12}$ receptor-deficient mice, indicating that rapid process extension is dependent on ATP sensed through microglial $P2Y_{12}$ receptors (Haynes et al., 2006). The involvement of $P2Y_{12}$ receptors in triggering microglial motility, i.e., chemotaxis, was originally found by Honda et al. (2001), in cultured microglia, which has recently been confirmed *in vivo* in $P2Y_{12}$ receptor-deficient animals (Haynes et al., 2006). Neuronal injury results in the release or leakage of ATP, which appears to function as a chemoattractant or "find-me" signal from damaged neurons to microglia (Fig. 1A). Recently, we have found that adenosine, a metabolite of ATP, acting on adenosine A_3 receptors, is also involved in the ATP-induced process extension (Ohsawa et al., 2012). Adenosine is released from cells or generated from extracellular ATP via breakdown by ENTPDases and CD73/5′-nucleotidase enzymes (Robson et al., 2006; Fig. 1A). Adenosine activates metabotropic adenosine A_1, A_{2A}, A_{2B}, and A_3 receptors, among which microglia from adult healthy brains express higher levels of A_1 and A_3 receptors (Fig. 1B). The released ATP seems to stimulate both $P2Y_{12}$ receptors as ATP/ADP and A_3 receptors as metabolized adenosine. Interestingly, simultaneous stimulation of both receptors is required for the process extensions, suggesting that there should be an intimate crosstalk between $P2Y_{12}$ and A_3 receptors in controlling the process extension (Fig. 1C). There are other molecules that could control the process extensions of microglia, such as glutamate, γ-aminobutyric acid (Fontainhas et al., 2011), and fractalkine (Liang et al., 2009). However, purinergic signals would be the primary system that triggers the process extension, because $P2Y_{12}$ receptors are highly expressed in both surveying and extending microglia (Fig. 1B), and the release or leakage of ATP is an initial event in cellular injury or death. The activation of P2 receptors often induces several chemokines, cytokines, and neurotransmitters, which may induce secondary effects on the microglial movement.

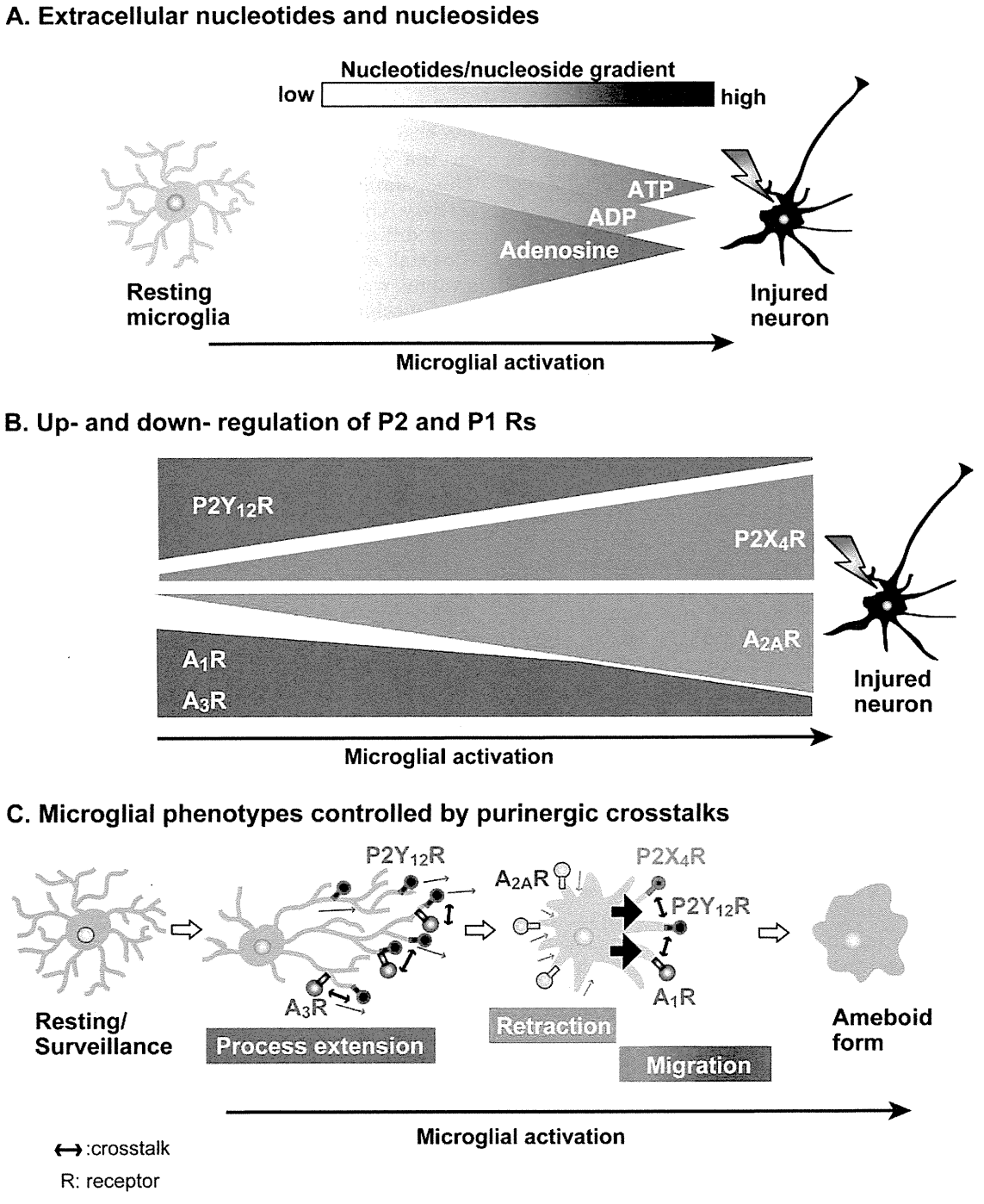

Fig. 1. $P2Y_{12}$ receptor-mediated process extension and migration in microglia, showing the effects of other P2 and P1 receptors. (**A**) Release/ leakage of nucleotides/nucleosides from injured neurons. When neurons or cells are injured or dead, high concentrations of ATP (~ mM) are leaked. The released ATP is diffused and also metabolized into ADP, AMP and adenosine. (**B**) Changes in P2 and P1 receptors involved in the motility of microglia. Resting microglia in the adult healthy brains express multiple P2 and P1 receptors. Within these receptors, $P2Y_{12}$, $P2X_4$, A_1, and A_3 receptors are thought to be important for the dynamic motility of microglia. When microglia are activated, they upregulate $P2X_4$ and A_{2A} receptors, whereas $P2Y_{12}$ receptors are decreased (in some cases, for example spinal microglia in a neuropathic pain model, these are increased). (**C**) Process extension, retraction and migration induced by P2 or P1 receptors. When resting/surveying microglia sense ATP/ADP by $P2Y_{12}$ receptors, they extend their processes to the injured sites. This event is cooperatively controlled by simultaneous activation of adenosine A_3 receptors by adenosine. Microglia upregulate adenosine A_{2A} receptors, by which they retract their processes and form round-shaped activated microglia. Activated microglia upregulate $P2X_4$ receptors, whereas decrease $P2Y_{12}$ receptors. Activation of $P2Y_{12}$ receptors by ATP/ADP in activated microglia resulted in migration toward the injured sites. Activation of $P2X_4$ receptors by ATP enhanced the microglial migration, suggesting positive crosstalk between $P2Y_{12}$ and $P2X_4$ receptors. The $P2Y_{12}$ receptor-mediated migration requires co activation of adenosine A_1 and $P2Y_{12}$ receptors, suggesting cooperative and essential crosstalk between these receptors for the migration.

With regard to the intracellular molecules that are responsible for the microglial process extension, we found that the ATP/ADP-induced process extension requires activations of the phosphatidylinositol 3′-kinase (PI3K) and phospholipase C (PLC) pathways, inhibition of the adenylate cyclase pathway downstream of $P2Y_{12}$ receptors, integrin-β1 activation and its accumulation in the tip of the extending processes (Ohsawa et al., 2010; Ohsawa and Kohsaka, 2011).

PROCESS-RETRACTING MICROGLIA

Activated microglia retract their processes during neurodegeneration and neuroinflammation, which is thought to be strongly correlated with the functional transformation of microglia into an activated or proinflammatory phenotype (Kreutzberg, 1996). Adenosine has been shown to induce process retraction and the repulsion of lipopolysaccharide (LPS)-activated microglia (Orr et al., 2009). The application of ATP to LPS-activated microglia causes chemorepulsive migration away from ATP and induces rapid process retraction. Microglia activated by LPS have been shown to retract their processes and to undergo repulsive migration in response to ATP, which is metabolized into adenosine and sensed through the Gs-protein-coupled adenosine A_{2A} receptor. Although the expression level of the adenosine A_{2A} receptor in surveying/resting microglia is quite low, LPS dramatically increases its expression, whereas, interestingly, it rather decreases $P2Y_{12}$ receptor expression in microglia (Haynes et al., 2006; Orr et al., 2009; Fig. 1B). This finding may explain, in part, the modal shift from the ramified to the amoeboid microglial morphology that is observed in some inflammatory states (Fig. 1C). The upregulation of A_{2A} expression is observed in pathological brains, such as those afflicted by Parkinson disease or ischemia (Pedata et al., 2001; Schwarzschild et al., 2006). The change in the balance of A_{2A} and $P2Y_{12}$ receptor expressions following nerve injury may be important for the regulation of microglial motility, including process extension and retraction, as well as migration.

MIGRATING MICROGLIA

Microglia are transformed into the "activated form" with the enlarged soma, retracted and shortened processes in traumatic or neurodegenerative diseases in the CNS. They also show an "ameboid" shape, appearing as rounded cells with spare processes. These activated microglia have high motility and can move through brain tissue. Various kinds of factors reportedly stimulate microglial cell migration, including chemokines, such as MCP-1 and fractalkine (Hayashi et al., 1995; Lauro et al., 2006), neurotrophic factors, such as NGF and EGF (Gilad and Gilad, 1995; Nolte et al., 1997), amyloid-β (Du Yan et al., 1997; Tiffany et al., 2001), complemental C5a (Yao et al., 1990), neuropeptide bradykinin (Ifuku et al., 2007), and neureglin-1 (Calvo et al., 2010). These molecules have important roles in regulating the neurotoxic or neuroprotective functions of microglia. Extracellular ATP and the activation of Gi/o-coupled $P2Y_{12}$ receptors, however, are also important for microglial chemotaxis and membrane ruffling (Honda et al., 2001). A study using $P2Y_{12}$ receptor-deficient mice has shown that primary-cultured microglia from $P2Y_{12}$ receptor-deficient mice did not exhibit ATP-induced membrane ruffling and chemotaxis, indicating that the $P2Y_{12}$ receptor is essential for the migration of microglia stimulated by ATP (Haynes et al., 2006). Similar to process extension, the activations of the PI3K and PLC pathways, PI3K/Akt activation (Irino et al., 2008; Ohsawa et al., 2007) and inhibition of adenylate cyclase pathways together with a decrease in the cyclic AMP level and protein kinase A (Nasu-Tada et al., 2005) are involved in the $P2Y_{12}$ receptor-mediated migration. Extracellular nucleotides function as "find-me" signal in peripheral tissues. Thymocytes at early stage of apoptosis release ATP/UTP to recruit monocytes/macrophages. However, the responsible receptor for the recruitment of monocytes is $P2Y_2$ receptor, and thus, their migration was dramatically decreased in monocytes obtained from $P2Y_2$ receptor-deficient mice (Elliott et al., 2009).

The $P2Y_{12}$ receptor-mediated microglial migration, however, is facilitated or modulated strongly by other P2 or P1 receptor-mediated signals. In animal models of neuropathic pain, the activation of spinal microglia is concomitant with the upregulation of $P2X_4$ receptors (Tsuda et al., 2003; Fig. 1B). The pharmacological blockade of $P2X_4$ receptors and RNA interference-based knockdown of the $P2X_4$ receptor in microglia suppressed microglial chemotaxis (Ohsawa et al., 2007). ATP causes an increase in the intracellular calcium concentration mainly by inducing extracellular Ca^{2+} influx through the $P2X_4$ receptor, which modulates the activation of the PI3K/Akt pathway in microglia, through which chemotactic responses could be facilitated. The $P2Y_{12}$ receptor is constitutively expressed in microglia in the normal brain (Sasaki et al., 2003), and its expression is upregulated in activated microglia following facial nerve axotomy or nerve injury in the spinal cord (Gamo et al., 2008; Tozaki-Saitoh et al., 2008), whereas it is rather decreased by kainic acid (KA) (Koizumi et al., 2007) in the hippocampus or by LPS in the cortex (Orr et al., 2009). In contrast, $P2X_4$ receptor expression in microglia is lower in the normal brain and spinal cord and is significantly upregulated in activated microglia within 24 h after ischemia or nerve injury and during the tactile allodynia observed after nerve injury (Cavaliere et al., 2003; Schwab et al., 2005; Tsuda et al., 2003, 2005; Fig. 1B). These observations suggest that $P2X_4$ receptor activation may modulate or enhance microglial cell migration under pathological conditions. In addition, adenosine has an essential role in the ATP-induced microglial migration. Although adenosine alone had no effect, the ATP failed to stimulate $P2Y_{12}$ receptor-mediated microglial migration in CD39/ENTPDase1- or A_1 receptor-deficient microglia (Farber et al., 2008). Interestingly, the

failure to migrate was restored by the addition of adenosine, an adenosine agonist or soluble ENTPDase. A similar observation was already made for neutrophils, where an ATP-induced chemotaxis in neutrophils requires co-stimulation with $P2Y_2$ and adenosine A_3 receptors (Chen et al., 2006). Thus, the ATP-induced microglial migration appears to be under the control of co-stimulation with $P2Y_{12}$ and adenosine A_1 receptors by ATP/ADP and adenosine respectively, though the precise molecular mechanisms remain unknown. All these findings suggest that there should be an intimate crosstalk among purinergic receptors for microglial migration when exposed to ATP. The released ATP itself and its metabolites by CD39 or CD73 differentially act on P2 and P1 receptors to cause migration. Microglia may change the expression levels of these receptors, ENTPDases, CD73/5′-nucleotidase enzymes, and thus regulate the purinergic signals and migratory responses.

PHAGOCYTIC MICROGLIA

Finally, we describe $P2Y_6$ receptor-mediated phagocytic microglia. When microglia migrate to and arrive at the injured sites, they would determine whether they should rescue the damaged cells or rather kill and phagocytose them. For this determination, UDP and activation of $P2Y_6$ receptors have indispensable roles. UDP is an endogenous agonist to the $P2Y_6$ receptor that is leaked when neurons are dead or injured. Activation of the $P2Y_6$ receptor results in a drastic increase in the motility of microglia, leading to engulfment and phagocytosis of the target molecules. Thus, UDP and the $P2Y_6$ receptor in microglia function as an "eat-me" signal and a phagocytosis receptor, respectively (Inoue et al., 2009; Kataoka et al., 2011; Kettenmann, 2007; Koizumi et al., 2007). Phagocytosis, a specialized form of endocytosis, is the uptake by a cell of relatively large particles (>1.0 μm) into phagosomes and is a central mechanism in tissue remodeling, inflammation, and the defense against infectious agents (Tjelle et al., 2000). Recognition is the first and most important step, and thus extensive studies on cell-surface phagocytosis receptors as well as the corresponding ligands (eat-me signals) have been reported, including Fc receptors, complement receptors, integrins, endotoxin receptors (CD18, CD14), mannose receptors, scavenger receptors (Lauber et al., 2003), and phosphatidylserine (PS) receptors, such as BAI-1 (Park et al., 2007) and Tim4 (Miyanishi et al., 2007). It seems to be difficult for phagocytes to recognize diffusible signals, such as nucleotides or UDP, simply because they quickly diffuse. However, UDP could be a potential "eat-me" signal because (i) release or leakage of UDP (released as UTP) induced by KA is estimated to be less than 10% that of ATP (Koizumi et al., 2007), and thus its diffusion would be localized (Fig. 2A); (ii) UDP is immediately degraded by ENTPDases, suggesting that extracellular UDP should be present transiently. This characteristic feature of UDP is suitable as an eat-me signal that could restrict the targets to be phagocytosed. In addition, the findings that UDP stimulated neither other P2 and P1 receptors (Fig. 2B, insert) nor chemotaxis, but instead caused only phagocytosis of microglia would be a useful character for the eat-me signal (Koizumi et al., 2007).

Resting microglia in the adult healthy brain show almost no expression of $P2Y_6$ receptors. In addition, as mentioned above, extracellular UDP is a spatiotemporally restricted signal. Thus, resting microglia in the healthy brains would have no chance to meet or sense UDP. When activated, however, microglia dramatically increased $P2Y_6$ receptors to become phagocytes, whereas they decreased $P2Y_{12}$ receptors (Inoue et al., 2009; Koizumi et al., 2007), i.e., there is a functional modal shift of the microglia from migrating to phagocytic. The mechanisms underlying the specific upregulation of $P2Y_6$ receptors on the microglia remain to be clarified. However, stimulation with various nucleotides nor nucleosides did not upregulate microglial $P2Y_6$ receptors (unpublished data), suggesting that molecules other than nucleotides/nucleosides would be important for the modal shift. It is interesting that UDP is not able to efficiently activate $P2Y_{12}$ receptors, nor is ATP/ADP able to act on $P2Y_6$ receptors. As mentioned above, although UDP is a spatiotemporally restricted signal, ATP/ADP are not. However, even if these nucleotides are leaked or released simultaneously, adenine and uridine nucleotides would regulate the microglial motilities, i.e., chemotaxis and phagocytosis, in a mutually exclusive but coordinated fashion (Fig. 2B,C).

The release or leakage of UDP (released as UTP) induced by KA is estimated to be less than 10% that of ATP, and its diffusion would show a restricted spatiotemporal pattern (Fig. 2A). Importantly, UDP had no effect on the $P2Y_{12}$ receptor-mediated migration, and ATP/ADP had no effect on the $P2Y_6$ receptor-mediated phagocytosis. Thus, migration and phagocytosis are differentially controlled by two distinct P2 receptors, i.e., the $P2Y_{12}$ and $P2Y_6$ receptors, respectively.

CONCLUSIONS

This article describes that extracellular nucleotides/nucleosides and purinergic receptors are the predominant molecules and sensors employed by microglia to transform themselves into different phenotypes in pathological conditions. It should be noted that microglia differentially sense extracellular molecules by their different P2 and P1 receptors. Each P2 or P1 receptor could sense extracellular nucleotides/nucleosides differentially by its own sensitivity to nucleotides/nucleosides or by distinguishing their chemical properties. In addition, microglia change the expression level of P2 and P1 receptors according to their activation stages, and therefore could change their sensitivities to the nucleotides/nucleosides.

With regard to microglial process extension and migration, the activation of $P2Y_{12}$ receptors by ATP (or ADP) has a predominant role. ATP released or leaked

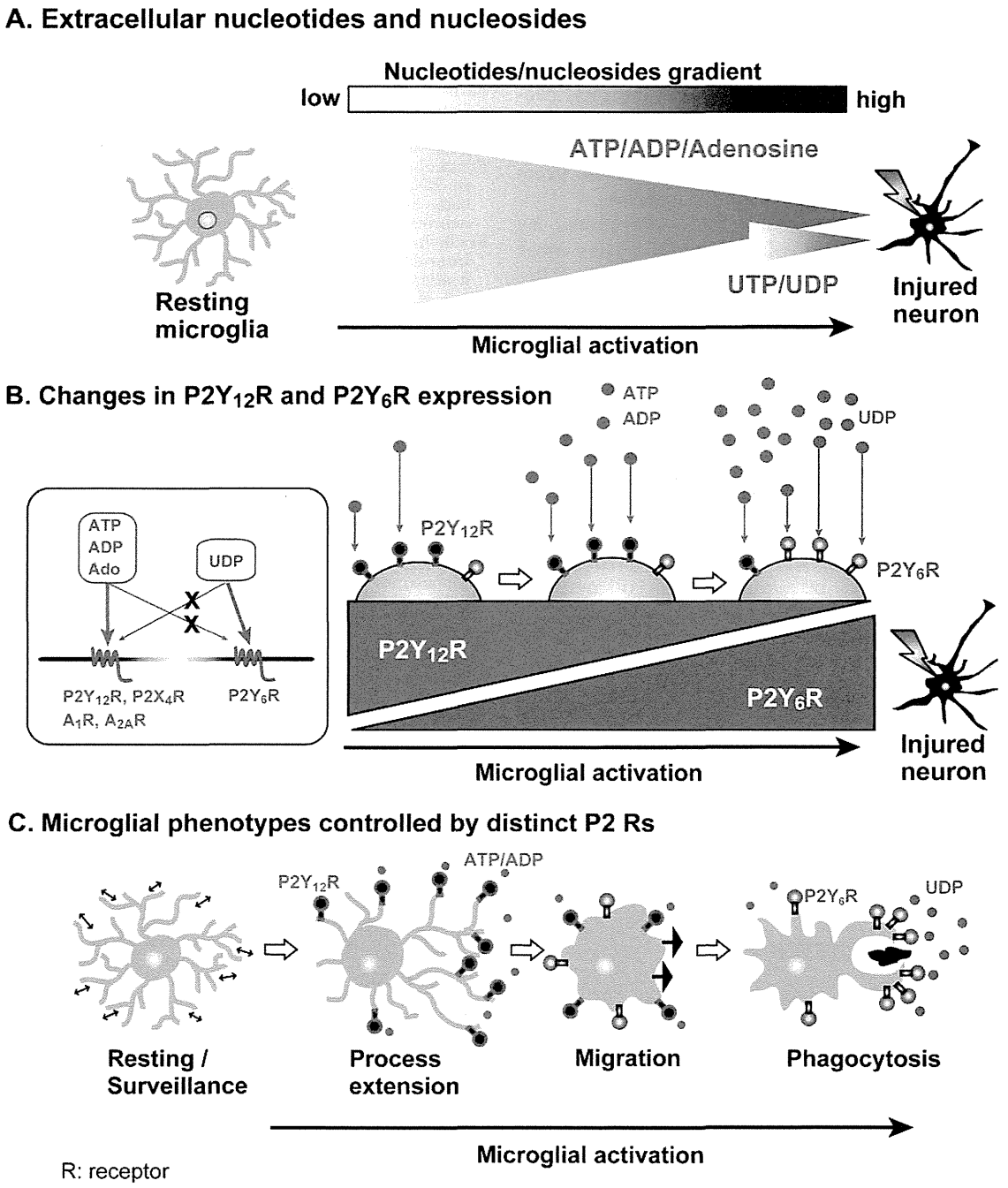

Fig. 2. Independence of $P2Y_{12}$ receptor-mediated migration and $P2Y_6$ receptor-mediated phagocytosis in microglia. (**A**) Release/leakage of adenine nucleotides/nucleosides, and uridine nucleotides from injured neurons. When neurons or cells are injured or dead, high concentrations of ATP ($\sim$ mM) and UTP at a concentration of less than 10% are leaked. Compared with ATP/ADP/adenosine, UTP/UDP should be transient and localized signals. (**B**) Changes in $P2Y_{12}$ and $P2Y_6$ receptors in microglia according to their activation stages. Insert shows pharmacological characterization of $P2Y_6$ receptor. UDP is a selective agonist to the $P2Y_6$ receptor, and thus it does not stimulate $P2Y_{12}$, $P2X_4$, A_1, or A_{2A} receptors. Similarly, the $P2Y_6$ receptor is a very selective receptor for UDP, and therefore is not activated by ATP, ADP or adenosine (Ado). Resting microglia express no or only faint $P2Y_6$ receptors whereas they express $P2Y_{12}$ receptors adequately. When microglia are activated, they increase $P2Y_6$ receptors, whereas they decrease $P2Y_{12}$ receptors. Only when activated microglia meet UDP at the injured sites, do they sense UDP as an eat-me signal. (**C**) Microglial migration and phagocytosis are controlled by distinct P2 receptors. When microglia sense ATP/ADP by $P2Y_{12}$ receptors, they extrude their processes, followed by migration toward the injured sites. These microglial motilities are not affected by UDP/$P2Y_6$ receptors. When activated, microglia upregulate $P2Y_6$ receptors and if they sense the eat-me signal UDP, they start to phagocytose the dead cells or debris. The phagocytic responses are not affected by the activation of $P2Y_{12}$ receptors nor by other P2 or P1 receptors.

from injured cells functions as a chemoattractant and induces microglial process extension, which is followed by microglial migration toward the injured sites. Multiple P2 and P1 receptors are involved in the ATP-induced responses and there should be an intimate crosstalk among these receptors for control or transformation of

this phenotype. Activation of $P2X_4$ receptors enhances the $P2Y_{12}$ receptor-mediated migration, whereas simultaneous activation of adenosine A_3 and A_1 receptors is essential for the $P2Y_{12}$ receptor-mediated microglial process extension and migration, respectively. Microglia upregulate adenosine A_{2A} receptors, the activation of which by adenosine rather causes retraction of the processes, forming round-shaped activated microglia.

Activated microglia upregulate $P2Y_6$ receptors, by which they phagocytose dead cells or debris if they meet UDP. UDP functions as an "eat-me" signal for $P2Y_6$ receptors. Interestingly, the $P2Y_6$ receptor-mediated responses are not affected by the activation of $P2Y_{12}$ receptors and vice versa, suggesting that eating and migrating behaviors are distinctively controlled by different purinergic receptors.

Other neurotransmitters also affect microglial motilities. For example, noradrenaline suppresses amyloid β(Aβ)-induced expression of proinflammatory factors, and increases cell migration and uptake of fibrillar Aβ (Heneka et al., 2010a). Thus, degeneration of locus ceruleus and subsequent noradrenaline deficiency increased inflammatory mediators, but reduced recruitment of microglial to Aβ plaque sites and microglial Aβ phagocytosis (Heneka et al., 2010b). However, ATP and other nucleotides/nucleosides are the first signals that enable microglia to sense brain injury or changes in the microenvironment of the brain. These signals initially affect microglial function and cause transformation of the microglial phenotypes, i.e., functional modal shifts. Cooperative or distinct purinergic signals appear to have indispensable roles in triggering the dynamic and complex modal shift of microglia.

REFERENCES

Boucsein C, Zacharias R, Farber K, Pavlovic S, Hanisch UK, Kettenmann H. 2003. Purinergic receptors on microglial cells: Functional expression in acute brain slices and modulation of microglial activation in vitro. Eur J Neurosci 17:2267–2276.

Burnstock G. 2006. Historical review: ATP as a neurotransmitter. Trends Pharmacol Sci 27:166–176.

Burnstock G, Fredholm BB, Verkhratsky A. 2011. Adenosine and ATP receptors in the brain. Curr Top Med Chem 11:973–1011.

Burnstock G, Verkhratsky A. 2009. Evolutionary origins of the purinergic signalling system. Acta Physiol (Oxf) 195:415–447.

Calvo M, Zhu N, Tsantoulas C, Ma Z, Grist J, Loeb JA, Bennett DL. 2010. Neuregulin-ErbB signaling promotes microglial proliferation and chemotaxis contributing to microgliosis and pain after peripheral nerve injury. J Neurosci 30:5437–5450.

Cavaliere F, Florenzano F, Amadio S, Fusco FR, Viscomi MT, D'Ambrosi N, Vacca F, Sancesario G, Bernardi G, Molinari M, Volontè C. 2003. Up-regulation of P2X2, P2X4 receptor and ischemic cell death: Prevention by P2 antagonists. Neuroscience 120:85–98.

Chen Y, Corriden R, Inoue Y, Yip L, Hashiguchi N, Zinkernagel A, Nizet V, Insel PA, Junger WG. 2006. ATP release guides neutrophil chemotaxis via P2Y2 and A3 receptors. Science 314:1792–1795.

Davalos D, Grutzendler J, Yang G, Kim JV, Zuo Y, Jung S, Littman DR, Dustin ML, Gan WB. 2005. ATP mediates rapid microglial response to local brain injury in vivo. Nat Neurosci 8:752–758.

Du Yan S, Zhu H, Fu J, Yan SF, Roher A, Tourtellotte WW, Rajavashisth T, Chen X, Godman GC, Stern D, et al. 1997. Amyloid-beta peptide-receptor for advanced glycation endproduct interaction elicits neuronal expression of macrophage-colony stimulating factor: A proinflammatory pathway in Alzheimer disease. Proc Natl Acad Sci USA 94:5296–5301.

Elliott MR, Chekeni FB, Trampont PC, Lazarowski ER, Kadl A, Walk SF, Park D, Woodson RI, Ostankovich M, Sharma P, et al. 2009. Nucleotides released by apoptotic cells act as a find-me signal to promote phagocytic clearance. Nature 461:282–286.

Farber K, Markworth S, Pannasch U, Nolte C, Prinz V, Kronenberg G, Gertz K, Endres M, Bechmann I, Enjyoji K, et al. 2008. The ectonucleotidase cd39/ENTPDase1 modulates purinergic-mediated microglial migration. Glia 56:331–341.

Fontainhas AM, Wang M, Liang KJ, Chen S, Mettu P, Damani M, Fariss RN, Li W, Wong WT. 2011. Microglial morphology and dynamic behavior is regulated by ionotropic glutamatergic and GABAergic neurotransmission. PLoS One 6:e15973.

Fredholm BB, IJzerman AP, Jacobson KA, Klotz KN, Linden J. 2001. International Union of Pharmacology. XXV. Nomenclature and classification of adenosine receptors. Pharmacol Rev 53:527–552.

Gamo K, Kiryu-Seo S, Konishi H, Aoki S, Matsushima K, Wada K, Kiyama H. 2008. G-protein-coupled receptor screen reveals a role for chemokine receptor CCR5 in suppressing microglial neurotoxicity. J Neurosci 28:11980–11988.

Gilad GM, Gilad VH. 1995. Chemotaxis and accumulation of nerve growth factor by microglia and macrophages. J Neurosci Res 41:594–602.

Halassa MM, Haydon PG. 2010. Integrated brain circuits: Astrocytic networks modulate neuronal activity and behavior. Annu Rev Physiol 72:335–355.

Hanisch UK, Kettenmann H. 2007. Microglia: Active sensor and versatile effector cells in the normal and pathologic brain. Nat Neurosci 10:1387–1394.

Hayashi M, Luo Y, Laning J, Strieter RM, Dorf ME. 1995. Production and function of monocyte chemoattractant protein-1 and other beta-chemokines in murine glial cells. J Neuroimmunol 60:143–150.

Haydon PG. 2001. GLIA: Listening and talking to the synapse. Nat Rev Neurosci 2:185–193.

Haynes SE, Hollopeter G, Yang G, Kurpius D, Dailey ME, Gan WB, Julius D. 2006. The P2Y12 receptor regulates microglial activation by extracellular nucleotides. Nat Neurosci 9:1512–1519.

Heneka MT, Nadrigny F, Regen T, Martinez-Hernandez A, Dumitrescu-Ozimek L, Terwel D, Jardanhazi-Kurutz D, Walter J, Kirchhoff F, Hanisch UK, et al. 2010a. Locus ceruleus controls Alzheimer's disease pathology by modulating microglial functions through norepinephrine. Proc Natl Acad Sci U S A 107:6058–6063.

Heneka MT, O'Banion MK, Terwel D, Kummer MP. 2010b. Neuroinflammatory processes in Alzheimer's disease. J Neural Transm 117:919–947.

Hines DJ, Hines RM, Mulligan SJ, Macvicar BA. 2009. Microglia processes block the spread of damage in the brain and require functional chloride channels. Glia 57:1610–1618.

Honda S, Sasaki Y, Ohsawa K, Imai Y, Nakamura Y, Inoue K, Kohsaka S. 2001. Extracellular ATP or ADP induce chemotaxis of cultured microglia through Gi/o-coupled P2Y receptors. J Neurosci 21:1975–1982.

Ifuku M, Farber K, Okuno Y, Yamakawa Y, Miyamoto T, Nolte C, Merrino VF, Kita S, Iwamoto T, Komuro I, et al. 2007. Bradykinin-induced microglial migration mediated by B1-bradykinin receptors depends on Ca2+ influx via reverse-mode activity of the Na+/Ca2+ exchanger. J Neurosci 27:13065–13073.

Inoue K. 2002. Microglial activation by purines and pyrimidines. Glia 40:156–163.

Inoue K, Koizumi S, Kataoka A, Tozaki-Saitoh H, Tsuda M. 2009. P2Y(6)-evoked microglial phagocytosis. Int Rev Neurobiol 85:159–163.

Irino Y, Nakamura Y, Inoue K, Kohsaka S, Ohsawa K. 2008. Akt activation is involved in P2Y12 receptor-mediated chemotaxis of microglia. J Neurosci Res 86:1511–1519.

James G, Butt AM. 2002. P2Y and P2X purinoceptor mediated Ca2+ signalling in glial cell pathology in the central nervous system. Eur J Pharmacol 447:247–260.

Kataoka A, Koga Y, Uesugi A, Tozaki-Saitoh H, Tsuda M, Inoue K. 2011. Involvement of vasodilator-stimulated phosphoprotein in UDP-induced microglial actin aggregation via PKC- and Rho-dependent pathways. Purinergic Signal 7:403–411.

Kettenmann H. 2007. Neuroscience: The brain's garbage men. Nature 446:987–989.

Kettenmann H, Hanisch UK, Noda M, Verkhratsky A. 2011. Physiology of microglia. Physiol Rev 91:461–553.

Kobayashi K, Fukuoka T, Yamanaka H, Dai Y, Obata K, Tokunaga A, Noguchi K. 2006. Neurons and glial cells differentially express P2Y receptor mRNAs in the rat dorsal root ganglion and spinal cord. J Comp Neurol 498:443–454.

Koizumi S, Fujishita K, Tsuda M, Shigemoto-Mogami Y, Inoue K. 2003. Dynamic inhibition of excitatory synaptic transmission by astrocyte-derived ATP in hippocampal cultures. Proc Natl Acad Sci U S A 100:11023–11028.

Koizumi S, Shigemoto-Mogami Y, Nasu-Tada K, Shinozaki Y, Ohsawa K, Tsuda M, Joshi BV, Jacobson KA, Kohsaka S, Inoue K. 2007. UDP acting at P2Y6 receptors is a mediator of microglial phagocytosis. Nature 446:1091–1095.

Kreutzberg GW. 1996. Microglia: A sensor for pathological events in the CNS. Trends Neurosci 19:312–318.

Lauber K, Bohn E, Krober SM, Xiao YJ, Blumenthal SG, Lindemann RK, Marini P, Wiedig C, Zobywalski A, Baksh S, et al. 2003. Apoptotic cells induce migration of phagocytes via caspase-3-mediated release of a lipid attraction signal. Cell 113:717–730.

Lauro C, Catalano M, Trettel F, Mainiero F, Ciotti MT, Eusebi F, Limatola C. 2006. The chemokine CX3CL1 reduces migration and increases adhesion of neurons with mechanisms dependent on the beta1 integrin subunit. J Immunol 177:7599–7606.

Liang KJ, Lee JE, Wang YD, Ma W, Fontainhas AM, Fariss RN, Wong WT. 2009. Regulation of dynamic behavior of retinal microglia by CX3CR1 signaling. Invest Ophthalmol Vis Sci 50:4444–4451.

Miyanishi M, Tada K, Koike M, Uchiyama Y, Kitamura T, Nagata S. 2007. Identification of Tim4 as a phosphatidylserine receptor. Nature 450:435–439.

Nakajima K, Reddington M, Kohsaka S, Kreutzberg GW. 1996. Induction of urokinase-type plasminogen activator in rat facial nucleus by axotomy of the facial nerve. J Neurochem 66:2500–2505.

Nasu-Tada K, Koizumi S, Inoue K. 2005. Involvement of beta1 integrin in microglial chemotaxis and proliferation on fibronectin: Different regulations by ADP through PKA. Glia 52:98–107.

Nimmerjahn A, Kirchhoff F, Helmchen F. 2005. Resting microglial cells are highly dynamic surveillants of brain parenchyma in vivo. Science 308:1314–1318.

Nolte C, Kirchhoff F, Kettenmann H. 1997. Epidermal growth factor is a motility factor for microglial cells in vitro: Evidence for EGF receptor expression. Eur J Neurosci 9:1690–1698.

Ohsawa K, Irino Y, Nakamura Y, Akazawa C, Inoue K, Kohsaka S. 2007. Involvement of P2X4 and P2Y12 receptors in ATP-induced microglial chemotaxis. Glia 55:604–616.

Ohsawa K, Irino Y, Sanagi T, Nakamura Y, Suzuki E, Inoue K, Kohsaka S. 2010. P2Y12 receptor-mediated integrin-beta1 activation regulates microglial process extension induced by ATP. Glia 58:790–801.

Ohsawa K, Kohsaka S. 2011. Dynamic motility of microglia: Purinergic modulation of microglial movement in the normal and pathological brain. Glia 59:1793–1799.

Ohsawa K, Sanagi T, Nakamura Y, Suzuki E, Inoue K, Kohsaka S. 2012. Adenosine A3 receptor is involved in ADP-induced microglial process extension and migration. J Neurochem 121:217–227.

Orr AG, Orr AL, Li XJ, Gross RE, Traynelis SF. 2009. Adenosine A(2A) receptor mediates microglial process retraction. Nat Neurosci 12:872–878.

Park D, Tosello-Trampont AC, Elliott MR, Lu M, Haney LB, Ma Z, Klibanov AL, Mandell JW, Ravichandran KS. 2007. BAI1 is an engulfment receptor for apoptotic cells upstream of the ELMO/Dock180/Rac module. Nature 450:430–434.

Pascual O, Ben Achour S, Rostaing P, Triller A, Bessis A. 2011. Microglia activation triggers astrocyte-mediated modulation of excitatory neurotransmission. Proc Natl Acad Sci U S A 109:E197–E205.

Pedata F, Corsi C, Melani A, Bordoni F, Latini S. 2001. Adenosine extracellular brain concentrations and role of A2A receptors in ischemia. Ann N Y Acad Sci 939:74–84.

Perea G, Araque A. 2010. GLIA modulates synaptic transmission. Brain Res Rev 63:93–102.

Pocock JM, Kettenmann H. 2007. Neurotransmitter receptors on microglia. Trends Neurosci 30:527–535.

Robson SC, Sevigny J, Zimmermann H. 2006. The E-NTPDase family of ectonucleotidases: Structure function relationships and pathophysiological significance. Purinergic Signal 2:409–430.

Sasaki Y, Hoshi M, Akazawa C, Nakamura Y, Tsuzuki H, Inoue K, Kohsaka S. 2003. Selective expression of Gi/o-coupled ATP receptor P2Y12 in microglia in rat brain. Glia 44:242–250.

Schwab JM, Guo L, Schluesener HJ. 2005. Spinal cord injury induces early and persistent lesional P2X4 receptor expression. J Neuroimmunol 163:185–189.

Schwarzschild MA, Agnati L, Fuxe K, Chen JF, Morelli M. 2006. Targeting adenosine A2A receptors in Parkinson's disease. Trends Neurosci 29:647–654.

Sperlagh B, Illes P. 2007. Purinergic modulation of microglial cell activation. Purinergic Signal 3:117–127.

Tiffany HL, Lavigne MC, Cui YH, Wang JM, Leto TL, Gao JL, Murphy PM. 2001. Amyloid-beta induces chemotaxis and oxidant stress by acting at formylpeptide receptor 2, a G protein-coupled receptor expressed in phagocytes and brain. J Biol Chem 276:23645–23652.

Tjelle TE, Lovdal T, Berg T. 2000. Phagosome dynamics and function. Bioessays 22:255–263.

Tozaki-Saitoh H, Tsuda M, Miyata H, Ueda K, Kohsaka S, Inoue K. 2008. P2Y12 receptors in spinal microglia are required for neuropathic pain after peripheral nerve injury. J Neurosci 28:4949–4956.

Tremblay ME, Stevens B, Sierra A, Wake H, Bessis A, Nimmerjahn A. 2011. The role of microglia in the healthy brain. J Neurosci 31:16064–16069.

Tsuda M, Inoue K, Salter MW. 2005. Neuropathic pain and spinal microglia: A big problem from molecules in "small" glia. Trends Neurosci 28:101–107.

Tsuda M, Shigemoto-Mogami Y, Koizumi S, Mizokoshi A, Kohsaka S, Salter MW, Inoue K. 2003. P2X4 receptors induced in spinal microglia gate tactile allodynia after nerve injury. Nature 424:778–783.

Wake H, Moorhouse AJ, Jinno S, Kohsaka S, Nabekura J. 2009. Resting microglia directly monitor the functional state of synapses in vivo and determine the fate of ischemic terminals. J Neurosci 29:3974–3980.

Yao J, Harvath L, Gilbert DL, Colton CA. 1990. Chemotaxis by a CNS macrophage, the microglia. J Neurosci Res 27:36–42.

Glycoconj J (2013) 30:247–256
DOI 10.1007/s10719-012-9435-9

Accumulation of free Neu5Ac-containing complex-type *N*-glycans in human pancreatic cancers

Masahiko Yabu · Hiroaki Korekane · Hidenori Takahashi · Hiroaki Ohigashi · Osamu Ishikawa · Yasuhide Miyamoto

Received: 25 June 2012 / Revised: 17 July 2012 / Accepted: 18 July 2012 / Published online: 14 August 2012

Abstract We have analyzed the structures of glycosphingolipids and intracellular free glycans in human cancers. In our previous study, trace amounts of free *N*-acetylneuraminic acid (Neu5Ac)-containing complex-type *N*-glycans with a single GlcNAc at each reducing terminus (Gn1 type) was found to accumulate intracellularly in colorectal cancers, but were undetectable in most normal colorectal epithelial cells. Here, we used cancer glycomic analyses to reveal that substantial amounts of free Neu5Ac-containing complex-type *N*-glycans, almost all of which were α2,6-Neu5Ac-linked, accumulated in the pancreatic cancer cells from three out of five patients, but were undetectable in normal pancreatic cells from all five cases. These molecular species were mostly composed of five kinds of glycans having a sequence Neu5Ac-Gal-GlcNAc-Man-Man-GlcNAc and one with the following sequence Neu5Ac-Gal-GlcNAc-Man-(Man-)Man-GlcNAc. The most abundant glycan was Neu5Acα2-6Galβ1-4GlcNAcβ1-2Manα1-3Manβ1-4GlcNAc, followed by Neu5Acα2-6Galβ1-4GlcNAcβ1-2Manα1-6Manβ1-4GlcNAc. This is the first study to show unequivocal evidence for the occurrence of free Neu5Ac-linked *N*-glycans in human cancer tissues. Our findings suggest that free Neu5Ac-linked glycans may serve as a useful tumor marker.

Keywords Free oligosaccharide · *N*-glycans · Pancreatic cancer · *N*-acetylneuraminic acid

Abbreviations

Neu5Ac	*N*-acetylneuraminic acid
SGP	Sialylglycopeptide
Cer	Ceramide
GM3	Neu5Acα3Galβ4GlcCer
LST-c	Neu5Acα6Galβ4GlcNAcβ3Galβ4GlcCer
GM1	Galβ3GalNAcβ4(Neu5Acα3)Galβ4GlcCer
LST-a	Neu5Acα3Galβ3GlcNAcβ3Galβ4GlcCer
Disialyl Lc_4	Neu5Acα3Galβ3(Neu5Acα6)GlcNAcβ3Galβ4GlcCer
SSEA-4	Neu5Acα3Galβ3GalNAcβ3Galα4Galβ4GlcCer
Disialyl SSEA-3	Neu5Acα3Galβ3(Neu5Acα6)GalNAcβ3Galα4Galβ4GlcCer

Introduction

Extensive studies on the oligosaccharide structures of cancers have revealed that aberrant glycosylation occurs in essentially all types of human cancers [1–4]. Altered carbohydrate determinants, including tumor associated carbohydrate antigens such as SLe^a and SLe^x have been utilized as useful tumor

Electronic supplementary material The online version of this article (doi:10.1007/s10719-012-9435-9) contains supplementary material, which is available to authorized users.

M. Yabu · Y. Miyamoto (✉)
Department of Immunology,
Osaka Medical Center for Cancer and Cardiovascular Diseases,
1-3-3 Nakamichi, Higashinari-ku,
Osaka 537-8511, Japan
e-mail: miyamoto-ya@mc.pref.osaka.jp

H. Korekane
Systems Glycobiology Research Group,
Chemical Biology Department, RIKEN Advanced Science Institute,
2-1 Hirosawa,
Wako, Saitama 351-0198, Japan

H. Takahashi · H. Ohigashi · O. Ishikawa
Department of Surgery,
Osaka Medical Center for Cancer and Cardiovascular Diseases,
1-3-3 Nakamichi, Higashinari-ku,
Osaka 537-8511, Japan

markers for the diagnosis of cancer [5–7]. Thus, the application of glycomic analyses to cancer research can highlight changes in the profiling of glycan structures during tumor development, leading to the identification of novel carbohydrate tumor markers. Hence, we comprehensively and precisely analyzed the structures of glycosphingolipids (GSLs) using highly purified colorectal cancer cells and normal colorectal epithelial cells from more than 60 patients and identified two kinds of novel tumor-associated carbohydrate antigens, Neu5Acα2-6(Fucα1-2)Galβ1-4GlcNAcβ1-3Galβ1-4Glc (α2-6-sialylated type 2H) and Neu5Acα2-6(Fucα1-2)Galβ1-3GlcNAcβ1-3Galβ1-4Glc (α2-6-sialylated type 1H), both of which are isomers of SLe^a and SLe^x [8–11]. The α2-6-sialylated type 2H was found in colorectal cancer cells from half of the cases, whilst α2-6-sialylated type 1H was specifically found in colorectal cancer cells from Lewis-negative patients. The suitability of these two carbohydrate antigens as tumor markers is currently being evaluated in our group.

In the present study, extensive structural analyses of oligosaccharides derived from pancreatic cancers have been undertaken. These analyses revealed the occurrence of substantial amounts of intracellular free Neu5Ac (*N*-acetylneuraminic acid)-containing complex-type *N*-glycans with a single GlcNAc at each reducing terminus in human pancreatic cancers. We observed both free glycans and GSLs in our assay. These molecules are extractable in chloroform-methanol solution, which was used to homogenize the cancer cells and tissues [12].

The occurrence of free high-mannose type *N*-glycans is well demonstrated in mammalian cells [13–15]. However, with the exception of mouse liver and two kinds of human stomach cancer derived cell lines (MKN7 and MKN45) [12, 16], free complex-type *N*-glycans, especially sialylated species, are not normally observed.

In our previous study, free Neu5Ac-containing complex-type *N*-glycans were found in colorectal cancers, but only at trace amounts [11]. However, a large amount of free Neu5Ac-containing complex-type *N*-glycans were found to accumulate in some pancreatic cancers. In this paper, the detailed structures of these free sialylated complex-type *N*-glycans that accumulate in human cancers are presented.

Materials and methods

The majority of the experimental procedures including purification of cancer cells and normal epithelial cells, isolation of GSLs and free oligosaccharides, preparation and separation of pyridylaminated (PA)-oligosaccharides, and mass spectrometry analyses have been reported previously [11]. In brief, pancreatic cancer cells and normal pancreatic epithelial cells were highly purified from primary lesions of pancreatic cancers and their surrounding normal pancreatic lesions, respectively, using the epithelial cell marker, CD326, and magnetic beads. CD326 positive cells were extracted with 1,200 μl of chloroform/methanol (2:1, v/v), followed by 800 μl of chloroform/methanol/water (1:2:0.8, v/v/v). This methodology extracts both GSLs and free oligosaccharides. The extracts were loaded onto a DEAE-Sephadex A25 column and flow-through fractions were collected as neutral oligosaccharides. Acidic oligosaccharides were subsequently eluted with 200 mM ammonium acetate in methanol. The neutral and acidic fractions were digested with endoglycoceramidase II from *Rhodococcus* Sp. (Takara Bio) to release the oligosaccharide portion from GSLs. Liberated oligosaccharides from GSLs and free oligosaccharides were then labeled with 2-aminopyridine (2-AP) [17].

PA-oligosaccharides were separated on a Shimadzu LC-20A HPLC system equipped with fluorescence detector. Normal phase HPLC was performed on a TSK gel Amide-80 column (0.2×25 cm, Tosoh). The molecular size of each PA-oligosaccharide is given in glucose units (Glc) based on the elution times of PA-isomaltooligosaccharides. Reversed phase HPLC was performed on a TSK gel ODS-80Ts column (0.2×15 cm, Tosoh). The retention time of each PA-oligosaccharide is given in glucose units based on the elution times of PA-isomaltooligosaccharides. Thus, a given compound on these two columns provides a unique set of Glc (amide) and Gu (ODS) values, which correspond to coordinates of the 2-D map. PA-oligosaccharides were analyzed by LC/ESI MS/MS according to our previously established procedures [9].

Glycosidase digestions

Linkage position of Neu5Ac to the terminal galactose was determined as described previously [9]. Briefly, Neu5Ac-linked PA-oligosaccharides were digested with 2 U/ml of α2,3-sialidase from *Salmonella typhimurium* (Takara Bio) in 100 mM sodium acetate buffer, pH 5.5, for 2 h at 37 °C. Under these conditions, α2,3-sialidase specifically digests α2-3-Neu5Ac linked to the terminal residue, but not Neu5Ac with an α2-6-linkage. However, under conditions using 10 U/ml for 16 h, even so-called α2,3-sialidase can hydrolyze α2-6-Neu5Ac linked to the terminal residue, but not Neu5Ac linked to a non-terminal residue.

Preparation of free Neu5Ac-containing complex-type *N*-glycans

Authentic PA-oligosaccharides required for the analysis of GSLs have been already obtained in our laboratory and are listed in Table 1. However, we had no authentic PA-oligosaccharides of free oligosaccharides, and they were not commercially available. Hence, authentic PA-oligosaccharides of free oligosaccharides required for this study were prepared enzymatically. The procedure is outlined in Fig. 1. PA-oligosaccharides were prepared from sialylglycopeptide (SGP) (Tokyo Chemical Industry) (Fig. 1) and the results are

Table 1 Structures and elution positions in HPLC of standard PA-oligosaccharides. Peak numbers shown in Fig. 2 are given in parentheses

Abbreviation	Structure	Elution position in HPLC	
		Size (Gu)	RP (Gu)
GM3 (G1)	Neu5Acα2-3Galβ1-4Glc-PA	2.46	3.00
LST-c (G2)	Neu5Acα2-6Galβ1-4GlcNAcβ1-3Galβ1-4Glc-PA	4.40	3.76
GM1 (G3)	Galβ1-3GalNAcβ1-4Galβ1-4Glc-PA 3 | Neu5Acα2	3.85	2.92
LST-a (G4)	Neu5Acα2-3Galβ1-3GlcNAcβ1-3Galβ1-4Glc-PA	4.01	4.69
Disialyl Lc_4 (G5)	Neu5Acα2-3Galβ1-3GlcNAcβ1-3Galβ1-4Glc-PA 6 | Neu5Acα2	4.52	5.54
SSEA-4 (G6)	Neu5Acα2-3Galβ1-3GalNAcβ1-3Galα1-4Galβ1-4Glc-PA	4.98	4.81
Disialyl SSEA-3 (G7)	Neu5Acα2-3Galβ1-3GalNAcβ1-3Galα1-4Galβ1-4Glc-PA 6 | Neu5Acα2	5.26	7.47
S1-4G-Hex	Neu5Acα2-6Galβ1-4GlcNAcβ1-2Manα1 \ 6 Manβ1-4GlcNAc-PA 3 / Manα1	6.11	6.55
S2-4G-Hex (F6)	Manα1 \ 6 Manβ1-4GlcNAc-PA 3 / Neu5Acα2-6Galβ1-4GlcNAcβ1-2Manα1	6.01	5.15
S1-4G-Hex-Man (F4)	Neu5Acα2-6Galβ1-4GlcNAcβ1-2Manα1 \ 6 Manβ1-4GlcNAc-PA	5.21	5.93
S2-4G-Hex-Man (F3-2)	Manβ1-4GlcNAc-PA 3 / Neu5Acα2-6Galβ1-4GlcNAcβ1-2Manα1	5.00	6.84

summarized in Table 1. Two hundred micrograms of SGP was digested with 0.5 U/ml of recombinant endoglycosidase F2 from *Elizabethkingia meningosepticum* (Merck) in 100 mM sodium acetate buffer, pH 4.5, for 16 h at 37 °C. The released Gn1-type oligosaccharide (designated as SGP-F2, Fig. 1) was labeled with 2-aminopyridine (PA-SGP-F2). To cleave either side of the mannose arm, PA-SGP-F2 was partially digested with 1 U/ml of α2,3-sialidase from *S. typhimurium* in 100 mM sodium acetate buffer pH 5.5, for 16 h at 37 °C. Under these conditions, even so-called α2,3-sialidase can partially hydrolyze α2-6-Neu5Ac linked to the terminal residue. Two kinds of single digested oligosaccharides (S1 and S2) were separated and collected by reversed phase HPLC. S1 and S2 were sequentially digested with 0.4 U/ml β1,4-galactosidase from *Streptococcus pneumonia* (Prozyme) in 100 mM sodium citrate buffer, pH 6.0, for 2 h at 37 °C, followed by 10 U/ml of β-*N*-acetylhexosaminidase from jack bean (Seikagaku Kogyo) in 100 mM sodium citrate buffer pH 5.0, for 16 h at 37 °C (S1-4G-Hex, and S2-4G-Hex). Linkage position of the non-reducing terminal mannose of the two oligosaccharides (S1-4G-Hex and S2-4G-Hex) was determined by utilizing the specificity of jack bean α-mannosidase. S1-4G-Hex and S2-4G-Hex were digested with jack bean α-mannosidase (Seikagaku Kogyo) at either 10 U/ml or 25 U/ml in 100 mM sodium acetate buffer pH 5.0 containing 2 mM $ZnCl_2$, for 16 h at 37 °C. At the lower concentration, R-Manα1-6(Manα1-3)Manβ1-4GlcNAcβ1-4GlcNAc but not R-Manα1-3(Manα1-6)Manβ1-4GlcNAcβ1-4GlcNA is susceptible, where R is not H or Man. The substrate specificity of this enzyme was described previously [18]. Digestion with a low concentration

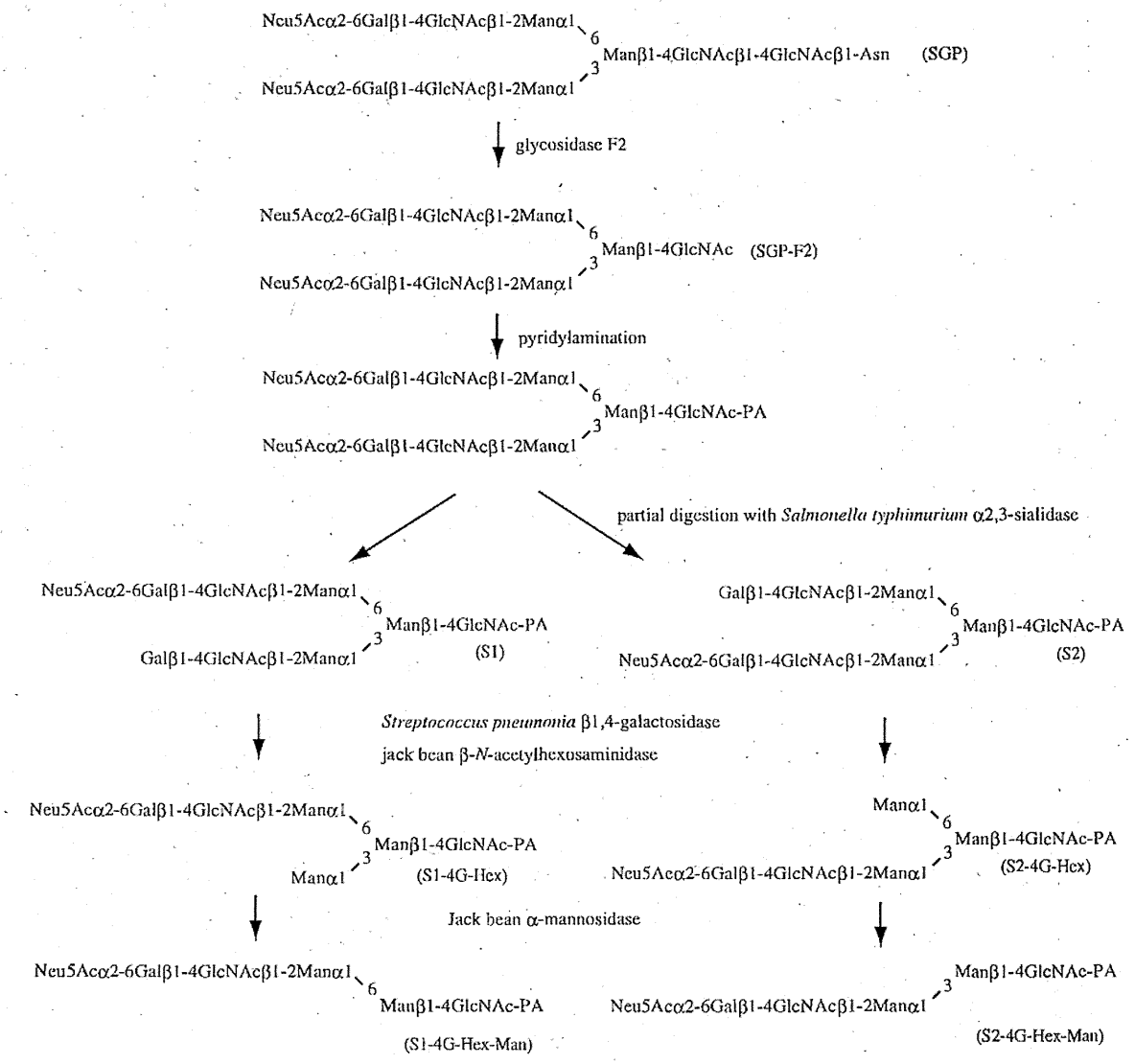

Fig. 1 The strategy used to synthesize authentic PA-free complex-type *N*-glycans

of α-mannosidase completely liberated the mannose residue from S1-4G-Hex (S1-4G-Hex-Man), indicating that the cleaved mannose was on the α1-3 side and the digested product (S1-4G-Hex-Man) was Neu5Acα2-6Galβ1-4GlcNAcβ1-2Manα1-6Manβ1-4GlcNAc-PA. S2-4G-Hex was partially cleaved by a high concentration of α-mannosidase, indicating that the cleaved mannose was on the α1-6 side and the digested product (S2-4G-Hex-Man) was Neu5Acα2-6Galβ1-4GlcNAcβ1-2Manα1-3Manβ1-4GlcNAc-PA.

Results

Preparation of PA-oligosaccharides from colon and pancreatic adenocarcinoma

Colon and pancreatic cancer cells and their normal epithelial cells were isolated with high purity from the cancer tissues and surrounding normal epithelial tissues using magnetic beads labeled with antibody against the epithelial cell marker, CD326. We analyzed the structures of GSLs and free oligosaccharides of pancreatic cancer cells and normal pancreatic cells derived from five patients. The clinicopathological features of the five pancreatic cancer patients are described in Supplementary Table 1.

It is well known that both free oligosaccharides and GSLs, but not glycoproteins, are recovered in lipid fractions from biological samples [12]. In this study, both free oligosaccharides and GSLs were extracted from the isolated cells using organic solvent, chloroform-methanol. The oligosaccharide portions of GSLs were released by endoglycoceramidase II, and the reducing ends of the released oligosaccharides of GSLs and free oligosaccharides were tagged with the fluorophore, 2-aminopyridine (see Materials and Methods).

Major acidic free oligosaccharides accumulated in human cancer cells

The acidic PA-oligosaccharides from cancer cells and normal epithelial cells were analyzed by size-fractionation HPLC (Fig. 2a–h). Each of the peaks separated by the size-fractionation HPLC was further separated by reversed phase HPLC. Additionally, the separated PA-oligosaccharides were subjected to LC/ESI MS^2 analysis. Some of the PA-oligosaccharides were also analyzed after digestion with glycosidase to help ascertain their structures. By means of these combinational analyses, the structures of all the major GSLs could be estimated and the occurrence of a large amount of free sialylated complex-type *N*-glycans in cancer cells was unequivocally demonstrated. In total, 7 distinct Neu5Ac-containing free oligosaccharides (F1, F2, F3-1, F3-2, F4, F5, and F6) were detected as major components in human pancreatic cancers (Fig. 2, Tables 2, 3). All these glycans were easily predicted to be Neu5Ac-containing free complex-type *N*-glycans having a single HexNAc (probably GlcNAc) at their reducing termini (Gn1 glycans) by mass analyses. Elution positions, mass data and estimated composition of the

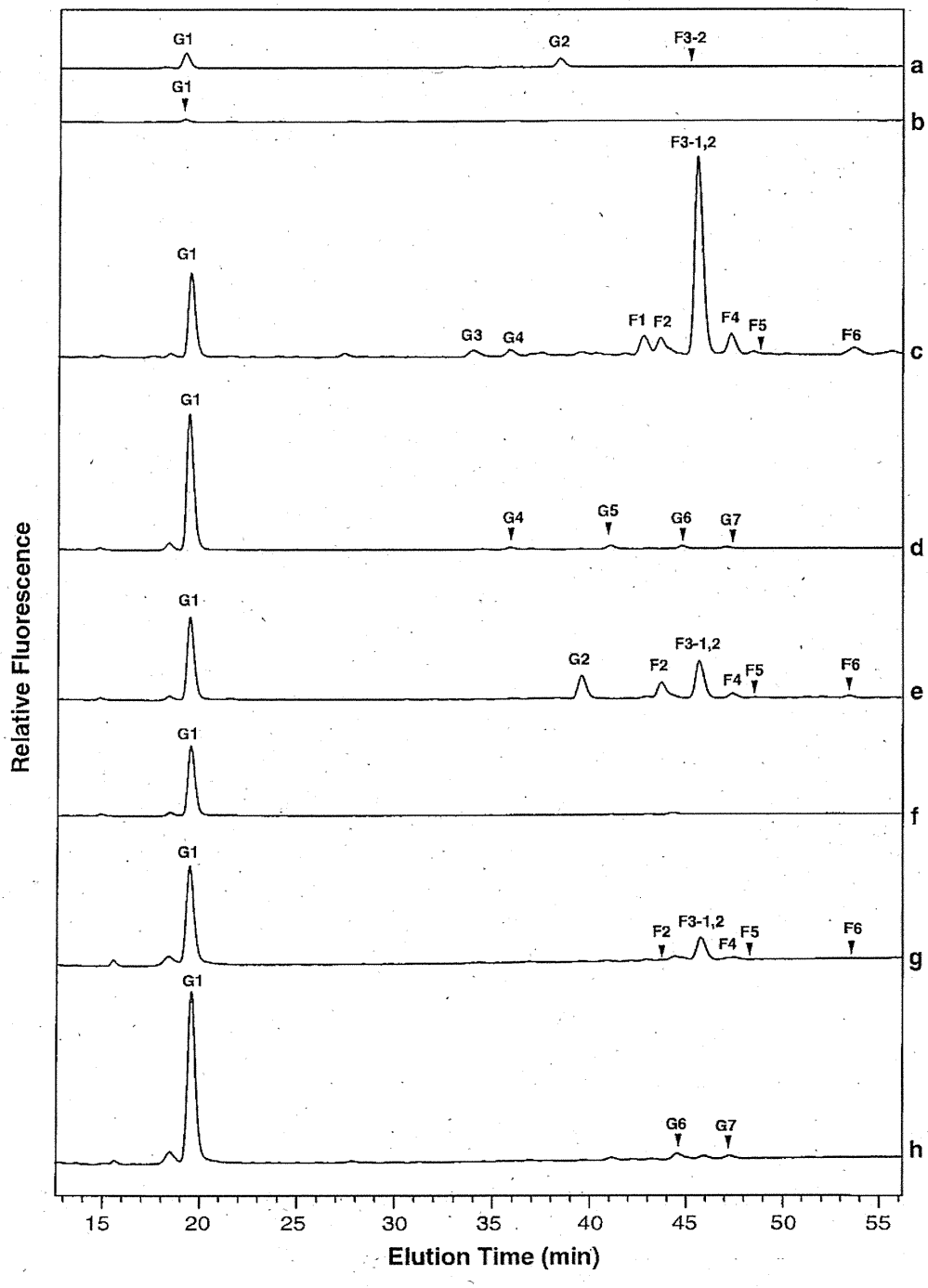

Fig. 2 Size fractionation HPLC of acidic PA-oligosaccharide mixtures obtained from human cancer and normal epithelial cells. **a** and **b** colon cancer cells (**a**) and normal colon epithelial cells (**b**) from the representative case (1×10^6 cells each), **c**–**h** pancreatic cancer cells (**c**, **e** and **g**) and normal pancreatic epithelial cells (**d**, **f** and **h**) (1×10^6 cells each). **c** and **d**, **e** and **f**, and **g** and **h** are from the same case (case 1, case 2 and case 3, respectively, Supplementary Table 1). Six major peaks derived from free *N*-glycans found in pancreatic cancer (**c**) are represented as F1–F6 with fraction numbers as per Tables 1, 2 and 3. Free *N*-glycan peaks found in other cells are numbered as per the peak numbers of C. G1–G7 are the peaks derived from GSLs. The structures of G1–G7 are listed in Table 1. The positions of minor peaks that were barely detectable are highlighted by an arrowhead

Table 2 Elution positions in HPLC and mass analysis of sialylated PA- free oligosaccharides obtained from human pancreatic cancer cells.

Group	Fraction	Elution position in HPLC		Mass (observed)	Mass (calculated)	Estimated composition
		Size (Gu)	RP (Gu)			
1	F3-1	5.03	5.55	1280.5	1280.5 $[M+H]^+$	$NeuAc_1Hex_3HexNAc_2$-PA
	F3-2	5.02	6.92	1280.4	1280.5 $[M+H]^+$	$NeuAc_1Hex_3HexNAc_2$-PA
	F4	5.26	6.00	1280.5	1280.5 $[M+H]^+$	$NeuAc_1Hex_3HexNAc_2$-PA
	F5	5.38	6.03	1280.5	1280.5 $[M+H]^+$	$NeuAc_1Hex_3HexNAc_2$-PA
	F1	4.76	7.91	1280.5	1280.5 $[M+H]^+$	$NeuAc_1Hex_3HexNAc_2$-PA
2	F6	6.07	5.20	1442.4	1442.5 $[M+H]^+$	$NeuAc_1Hex_4HexNAc_2$-PA
3	F2	4.84	7.80	1321.5	1321.5 $[M+H]^+$	$NeuAc_1Hex_2HexNAc_3$-PA

oligosaccharides are presented in Table 2. Based on the composition of monosaccharide, we were able to classify the 7 free *N*-glycans into three groups as follows; group 1 (F1, F3-1, F3-2, F4 and F5), group 2 (F6), and group 3 (F2) (Tables 2, 3). In the following results sections, the structures of these PA-oligosaccharides are explained in detail.

Structural analyses of free Neu5Ac-containing complex-type N-glycans

Group 1

The $MS^{1,2}$ spectra of the five group 1 glycans (F1, F3-1, F3-2, F4 and F5) were essentially the same. A representative $MS^{1,2}$ spectrum of F3-2 is shown in Fig. 3a, b. The structures of group 1 *N*-glycans were judged to be Neu5Ac-Hex-HexNAc-Hex-Hex-HexNAc-PA or branched Neu5Ac-HexNAc-Hex-(Hex-)Hex-HexNAc-PA by MS^2 analysis (Fig. 3a, b, Table 3), and they were anticipated to be Neu5Ac-Gal-GlcNAc-Man-Man-GlcNAc-PA or Neu5Ac-GlcNAc-Man-(Man-)Man-GlcNAc-PA, respectively. However, the latter candidate could be excluded because these oligosaccharides were resistant to jack bean α-mannosidase (data not shown). Neu5Ac is linked *via* α2-6 to the non-reducing terminal residue of F3-1, F3-2, F4 and F5, and α2-3 to that of F1 as determined by the specificity of α2-3-siallidase digestion as described in Material and Methods (Fig. 4, Table 3). These data suggested that two of the four oligosaccharides (F3-1, F3-2, F4 and F5) are

Table 3 Neu5Ac-containing free complex-type *N*-glycans accumulated in human cancers. Estimated structures and the amount of glycans in colon cancer cells (case of Fig. 2a), pancreatic cancer cells (cases of Fig. 2c, 2e, and 2g) are presented. The amount of glycan is expressed as pmol/1 $\times 10^6$ cells. (–) indicates that this glycan was not detected in the cells

Group	Fraction	Structure	Amount of glycan (pmol/1 X 10^6 cells) colon (A)	pancreas (C)	pancreas (E)	pancreas (G)
1	F3-1	Neu5Acα2-6Galβ1-4GlcNAcβ-Manα–Manβ1-4GlcNAc-PA	(-)	10.3	1.7	0.7
	F3-2	Neu5Acα2-6Galβ1-4GlcNAcβ1-2Manα1 / 3 Manβ1-4GlcNAc-PA	0.1	121.1	22.3	17.6
	F4	Neu5Acα2-6Galβ1-4GlcNAcβ1-2Manα1 \ 6 Manβ1-4GlcNAc-PA	(-)	16.6	2.9	1.9
	F5	Neu5Acα2-6Galβ1-4GlcNAcβ-Manα–Manβ1-4GlcNAc-PA	(-)	0.9	0.9	0.3
	F1	Neu5Acα2-3Galβ1-4GlcNAcβ1-2Manα1 / 3 Manβ1-4GlcNAc-PA	(-)	6.9	(-)	(-)
2	F6	Neu5Acα2-6Galβ1-4GlcNAcβ1-2Manα1 / 3 Manα1 \ 6 Manβ1-4GlcNAc-PA	(-)	2.8	1.0	0.5
3	F2	Neu5Acα2-6HexNAc-GlcNAcβ-Manα–Manβ1-4GlcNAc-PA	(-)	8.9	8.4	0.5